Ocean Sci., 6, 837–859, 2010
www.ocean-sci.net/6/837/2010/
doi:10.5194/os-6-837-2010

Ocean Science

On the seasonal cycles and variability of Florida Straits, Ekman and Sverdrup transports at 26° N in the Atlantic Ocean

C. P. Atkinson[1], **H. L. Bryden**[1], **J. J-M. Hirschi**[1], **and T. Kanzow**[1,2]

[1]National Oceanography Centre, European Way, Southampton, SO14 3ZH, UK
[2]Ozeanzirkulation und Klimadynamik, Leibniz-Institut für Meereswissenschaften an der Universität Kiel, Düsternbrooker Weg 20, 24105 Kiel, Germany

Received: 20 April 2010 – Published in Ocean Sci. Discuss.: 29 April 2010
Revised: 10 August 2010 – Accepted: 17 September 2010 – Published: 1 October 2010

Abstract. Since April 2004 the RAPID array has made continuous measurements of the Atlantic Meridional Overturning Circulation (AMOC) at 26° N. Two key components of this system are Ekman transport zonally integrated across 26° N and western boundary current transport in the Florida Straits. Whilst measurements of the AMOC as a whole are somewhat in their infancy, this study investigates what useful information can be extracted on the variability of the Ekman and Florida Straits transports using the decadal timeseries already available. Analysis is also presented for Sverdrup transports zonally integrated across 26° N.

The seasonal cycles of Florida Straits, Ekman and Sverdrup transports are quantified at 26° N using harmonic analysis of annual and semi-annual constituents. Whilst Sverdrup transport shows clear semi-annual periodicity, calculations of seasonal Florida Straits and Ekman transports show substantial interannual variability due to contamination by variability at non-seasonal frequencies; the mean seasonal cycle for these transports only emerges from decadal length observations. The Florida Straits and Ekman mean seasonal cycles project on the AMOC with a combined peak-to-peak seasonal range of 3.5 Sv. The combined seasonal range for heat transport is 0.40 PW.

The Florida Straits seasonal cycle possesses a smooth annual periodicity in contrast with previous studies suggesting a more asymmetric structure. No clear evidence is found to support significant changes in the Florida Straits seasonal cycle at sub-decadal periods. Whilst evidence of wind driven Florida Straits transport variability is seen at sub-seasonal and annual periods, a model run from the 1/4° eddy-permitting ocean model NEMO is used to identify an important contribution from internal oceanic variability at sub-annual and interannual periods. The Ekman transport seasonal cycle possesses less symmetric structure, due in part to different seasonal transport regimes east and west of 50 to 60° W. Around 60% of non-seasonal Ekman transport variability occurs in phase section-wide at 26° N and is related to the NAO, whilst Sverdrup transport variability is more difficult to decompose.

Correspondence to: C. P. Atkinson
(christopher.atkinson@noc.soton.ac.uk)

1 Introduction

The Atlantic Meridional Overturning Circulation (AMOC) is a fundamental part of Earth's climate system which in combination with the horizontal wind-driven gyres transports large amounts of heat into the high northern latitudes. A substantial weakening of the AMOC is predicted in response to anthropogenic related changes in high latitude buoyancy flux (IPCC, 2007) and it is suggested that a total shutdown of the AMOC would have profound implications for the climate of northwest Europe (Vellinga and Wood, 2002). The RAPID-WATCH (formerly RAPID) array combines satellite wind stress observations (to obtain Ekman transports), Florida Current cable measurements and mid-ocean geostrophic transports (calculated from moored temperature, salinity and current sensors at the basin margins) to continuously monitor the strength of the AMOC at 26° N (Cunningham et al., 2007). These independent measurements have been shown to successfully resolve the AMOC at 26° N at timescales longer than 10 days (Kanzow et al., 2007).

Published by Copernicus Publications on behalf of the European Geosciences Union.

Since measurements began in April 2004, the RAPID-WATCH array has revealed that large AMOC variability exists at sub-seasonal to annual timescales (Cunningham et al., 2007; Kanzow et al., 2010). A present challenge for RAPID-WATCH is to separate climatically relevant AMOC variability from other more localised signal noise. Whilst only 4–5 years of mid-ocean transports are available, high quality decadal datasets are already available for both the Florida Straits and Ekman transport components of the array. It is the properties of these decadal timeseries that will form the focus of this study.

The Florida Current forms an upstream extension of the Gulf Stream and is constrained by the narrow, approximately 90 km wide Florida Straits. The Florida Current is both part of the western boundary current system of the North Atlantic subtropical gyre and a pathway for warm-water return flow of the Atlantic thermohaline circulation (Schmitz and Richardson, 1991). Mass transport through the Florida Straits has been almost continuously measured since April 1982 using a succession of submerged telephone cables located between 26° N–27° N (Larsen, 1992; Baringer and Larsen, 2001; Meinen et al., 2010). These observations began during the Sub Tropical Atlantic Climate Studies (STACS) program which ran from 1982–1984 and used a variety of measurement techniques to study the Florida Current (Molinari et al., 1985). Amongst many other results, STACS revealed that Florida Straits transport variability has a near continuous power spectrum and an apparent asymmetric seasonal cycle with a range of several Sverdrups. Prompted by this intensive period of observations, many studies of transport in the Florida Straits have followed the STACS era and a significant body of literature now exists on the Florida Current.

The relationship between Florida Straits transport variability and North Atlantic wind field variability has received considerable attention. On annual and sub-annual timescales, several links have been made between the Florida Current and both local and remote wind forcing (e.g. Schott and Zantopp, 1985; Leaman et al., 1987; Schott et al., 1988; Lee and Williams, 1988; Mayer and Weisberg, 1993) in general agreement with model results (e.g. Anderson and Corry, 1985a; Rosenfeld et al., 1989; Greatbatch and Goulding, 1989; Boning et al., 1991; Fanning et al., 1994; Greatbatch et al., 1995). A significant fraction of variance at these periods has been linked to local meridional wind stress forcing in the Florida Straits, particularly at periods of days to tens of days where a barotropic response occurs (Lee and Williams, 1988). Wind stress forcing local and downstream to the Florida Straits has also been implicated in driving the Florida Straits seasonal transport cycle. At annual (and sub-annual) period, the Florida Straits transport does not adjust to wind stress forcing eastward over the interior ocean (Anderson and Corry, 1985b), instead reflecting a combination of sources originating closer to the continental shelf. These include barotropic long topographic waves (generated by changes in $\mathrm{curl}_z(\boldsymbol{\tau}/h)$ along f/h contours) and baroclinic coastally trapped waves (Anderson and Corry, 1985a). Observations of the vertical structure of the Florida Current have shown that the seasonal cycle possesses both barotropic and baroclinic components (Leaman et al., 1987; Schott et al., 1988). At sub-monthly periods, some Florida Current variability has been related to meandering modes (Johns and Schott, 1987) and frontal eddies along the East Florida shelf (Lee et al., 1991; Fiechter and Mooers, 2003) while at much longer decadal timescales, Florida Straits transport appears to adjust to changes in wind stress curl over the sub-tropical gyre (Anderson and Corry, 1985b; DiNezio et al., 2009) and may respond to changes in Atlantic thermohaline circulation.

Ekman transport at 24° N has a weak seasonal cycle due to the proximity of a node in the seasonal cycle of wind stress (Jayne and Marotzke, 2001). Observations (Kanzow et al., 2009) and model studies (e.g. Sime et al., 2006; Hirschi et al., 2007) suggest that at sub-annual periods, barotropic compensation of Ekman transport is particularly important for AMOC variability in the sub-tropical latitudes. At 24° N, Ekman transport shows reasonable correlation to the North Atlantic Oscillation (NAO, Josey et al., 2002). The NAO (e.g. Hurrell et al., 2003) is a dominant mode of Sea Level Pressure (SLP) variability in the North Atlantic at monthly to interannual (and longer) timescales; during positive NAO conditions, SLP over the Azores is higher than normal which is generally associated with a strengthening of both westerly and trade winds. The NAO accounts for the largest amount of interannual variability in monthly North Atlantic SLP in all but 4 months of the year and is most pronounced in amplitude and areal coverage during Winter (Marshall et al., 2001). Atmospheric circulation variability in the form of the NAO arrises from the internal non-linear dynamics of the extratropical atmosphere and the predictability of seasonal to interannual NAO variability will most likely remain low (Hurrell et al., 2006; Hurrell and Deser, 2009).

This paper presents a detailed investigation of Florida Straits and Ekman transport properties at 26° N prompted by the presence of the RAPID-WATCH array. Some attention is also given to Sverdrup transport (wind stress curl) variability at 26° N which is a possible driver of AMOC variability. Whilst much is already known about Florida Current transport variability, this study aims to re-visit, update and expand upon some of the previous observations in light of the longer Florida Straits transport timeseries and modern wind stress climatologies that are now available. Ekman and Sverdrup transport variability at 26° N is described more thoroughly than in previous studies and where possible placed in the context of wider North Atlantic variability. This study mostly concentrates on sub-annual, seasonal and interannual timescales of variability which complement the observations currently being reported by RAPID-WATCH investigations.

This paper is organised as follows: firstly the data and methods used are outlined in Sect. 2; Sect. 3 describes and discusses properties of Florida Straits, Ekman and Sverdrup transports at 26° N and where possible places these in the context of wider North Atlantic wind stress variability (model data is also used in an attempt to understand Florida Straits transport variability at sub-annual to interannual periods); Sect. 4 further discusses seasonal variability and considers the results in the context of the AMOC; a summary of the main results is presented in Sect. 5.

2 Data and methods

2.1 Data

Daily Florida Straits cable transports for the period 1982–2007 were downloaded from the Atlantic Oceanographic and Meteorological Laboratory web page which are freely available, funded by the NOAA Office of Climate Observations (www.aoml.noaa.gov/phod/floridacurrent/, note that an approximately 20-month gap exists in the data from 1998–2000). Whilst seasonal cycles were analysed using raw daily data wherever possible, some timeseries analysis (e.g. power spectra) uses simple linear interpolation to fill data gaps where required. Monthly mean Florida Straits transports are produced from the daily data following DiNezio et al. (2009), where means calculated from less than 15 daily observations are not used and instead are estimated using linear interpolation.

Daily and monthly Ekman and Sverdrup transports at 26° N were calculated for the period 1980–2007 using gridded surface wind stress fields from the NCEP-NCAR reanalysis project (Kalnay et al., 1996; Kistler et al., 2001) which are freely available via the IRI/LDEO Climate Data Library (http://iridl.ldeo.columbia.edu/). Ekman and Sverdrup transports were calculated at latitude 25.71° N (note that grid spacing = 1.875° longitudinally and 1.905° latitudinally in the low and mid-latitudes).

Meridional Ekman transport across a grid cell, Ek_y, was calculated using:

$$\mathrm{Ek}_y(i,j) = -(f\rho_w)^{-1} L_x \tau_x(i,j), \tag{1}$$

where $f = 2\Omega\sin\Theta$ is the Coriolis parameter (with $\Omega = 7.292 \times 10^{-5}$ rad s^{-1} and latitude Θ = 25.71° N), ρ_w = density of sea water in the Ekman layer assumed to be 1024 kg m^{-3}, L_x = zonal dimension of a grid cell (m) and τ_x = climatological zonal wind stress (N m^{-2}). The longitude and latitude of a given grid point are denoted by indices (i, j).

Sverdrup transport across a grid cell, $\mathrm{Svd}(i,j)$, was calculated using:

$$\mathrm{Svd}(i,j) = \left(\frac{\partial f}{\partial y}\rho_w\right)^{-1} L_x \mathrm{curl}_z\boldsymbol{\tau}(\boldsymbol{i},\boldsymbol{j}), \tag{2}$$

where $\partial f/\partial y$ is meridional gradient of the Coriolis parameter (taken as 2.06×10^{-11}m^{-1} s^{-1}) and $\mathrm{curl}_z\tau$ is the wind stress curl calculated using a simple centered finite difference scheme following Josey et al. (2002):

$$\mathrm{curl}_z\boldsymbol{\tau}(\boldsymbol{i},\boldsymbol{j}) = \frac{\tau_y(i+1,j)-\tau_y(i-1,j)}{2L_x} - \frac{\tau_x(i,j+1)-\tau_x(i,j-1)}{2L_y} \tag{3}$$

Ekman and Sverdrup transports are then zonally integrated across 26° N over the ranges 76.875–15° W and 76.875–16.875° W respectively (where the reduced Sverdrup range avoids using land grid points).

In addition to NCEP-NCAR data, wind stresses from the 1° gridded NOC v1.1 climatology (1980–2005, available monthly from http://www.noc.soton.ac.uk/noc_flux/noc1_1.php, Josey et al., 2002) and 0.5° gridded IFREMER MWF QuikSCAT climatology (2000–2007, available daily and monthly from ftp.ifremer.fr/ifremer/cersat/products/gridded/mwf-quikscat/) were also used for comparison with the Florida Straits transports and in calculation of Ekman and Sverdrup transports at 26° N. NCEP-NCAR data is determined on a dynamical model and data assimilation system, whilst NOC and QuikSCAT are determined based on ship meteorological reports and satellite scatterometer data respectively. These three datasets therefore provide complementary methods for estimating the North Atlantic wind stress field and should help mitigate against sampling, measurement or methodological errors associated with any particular dataset. It should be noted that the NCEP-NCAR climatology assimilates QuikSCAT data where available and therefore these two datasets cannot strictly be considered independent.

The NAO index used in this study is based on periodically updated data distributed by NOAA's Climate Prediction Center (http://www.cpc.noaa.gov/products/precip/CWlink/pna/nao.shtml). This is a monthly index derived following the method of Barnston and Livezey (1987), based on a rotated principal component analysis that isolates the primary teleconnection patterns of the NAO using year-round (not just winter) data.

Monthly timeseries for Florida Straits, NCEP-NCAR Ekman and Sverdrup transports, NAO index and upper ocean transports measured by RAPID-WATCH are shown in Fig. 1. Mean transports and variability are also given.

2.2 Methods

The seasonal cycles shown in Fig. 2 are a composite of simple arithmetic daily means (e.g. mean of all January 1st's, January 2nd's etc), with standard error given as std. dev. of daily values divided by the square root of the number of observations. These are smoothed using a 5th order low-pass Butterworth filter with cut-off period 30 days (and mean

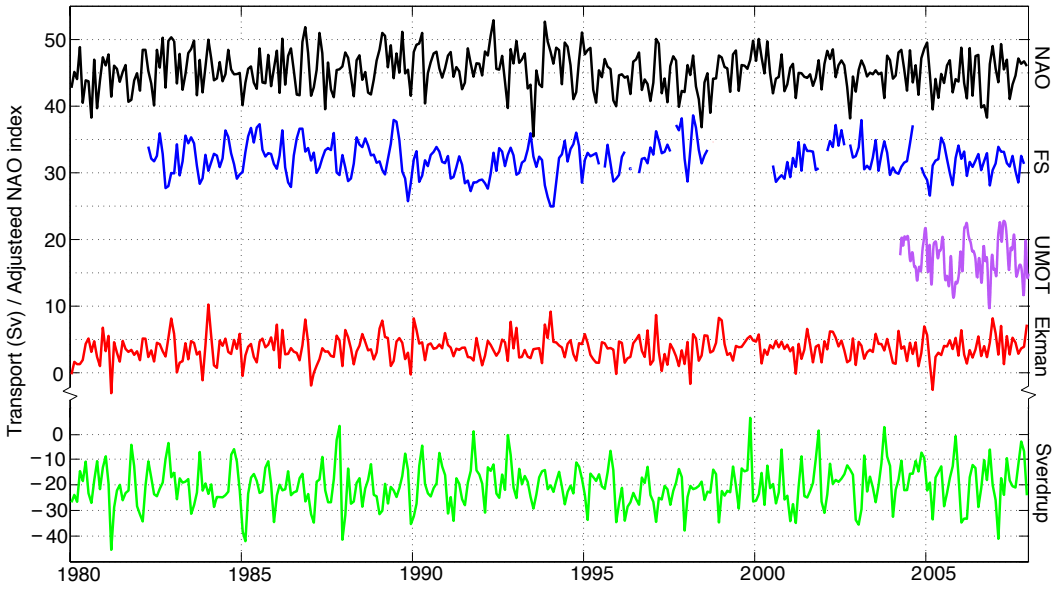

Fig. 1. Monthly timeseries of adjusted NAO index (black, 3×NAO index +15), Florida Straits transport (blue), 26° N southward upper mid-ocean transport (purple), 26° N NCEP Ekman transport (red, 76.875–15° W), 26° N NCEP Sverdrup transport (green, 76.875–16.875° W). Note change in scale size for Sverdrup transport. For transports: mean ± std. dev. is 32.1 ± 2.4 (3.3), 17.3 ± 2.8, 3.6 ± 1.9 (3.5) and −20.3 ± 8.0 (16.1) respectively (parentheses give std. dev. of daily timeseries where available).

transport subsequently removed). All low and high pass filtering (including seasonal cycles) is carried out using a 5th order Butterworth bandpass filter with no phase shifting in the time domain. Care was taken to avoid spurious filter edge effects associated with filtering by removing one filter width from each end of the filtered timeseries. Details of seasonal cycle harmonic analysis used in this study are given in Table 1 and Fig. 3.

Prior to timeseries analysis, means and linear trends were removed from the data. Power spectra were calculated using the Welch method, with data split into 8 sub-segments overlapping by 50% and a Hamming window applied. For clarity, 95% confidence limits are not shown on plots as broadly only the general character of the spectra is discussed (with the exception of annual and semi-annual peaks). Power spectra used during coherence analysis were calculated using an identical approach. Coherence significance levels were calculated using a simple bootstrap analysis, where one timeseries is randomly sampled prior to calculation of the coherence. This procedure was repeated 100 times and the 95th percentile of coherence values at each frequency found. Values of the 95th percentile were then averaged across all frequencies to give a base level of coherence attributable to random noise. Above this coherence is deemed 95% significant. Confidence limits calculated using this approach are in close agreement with theoretical limits based on estimates of the available degrees of freedom (Emery and Thomson, 2001).

3 Results

3.1 Florida Straits transport

3.1.1 Observations of the seasonal cycle

The mean seasonal cycle of transport through the Florida Straits for the period 1982–2007 is shown in Fig. 2a (bold red line). The seasonal cycle reaches a maximum of +1.6 Sv in mid-July, a minimum of −1.7 Sv in mid-January and shows a clear annual periodicity. Fitting annual and semi-annual harmonic components to the mean seasonal cycle (Fig. 3a) shows that the annual harmonic captures the structure of the mean seasonal cycle (root mean square (rms) error = 0.5 Sv) and that only a minor semi-annual component is present. The amplitudes of the annual and semi-annual harmonic components are 1.17 Sv and 0.19 Sv respectively (Table 1).

To investigate the year to year stability of the Florida Straits seasonal cycle, annual and semi-annual harmonics were also calculated for each year of the 1982–2007 Florida Straits transport record (excluding 1998 and 1999 where little data are available). The phases and amplitudes of these harmonic components (including those of the mean seasonal cycle) are presented in Fig. 3b-c where both annual and semi-annual harmonic components show clear interannual variability about the 1980–2007 means (bold black crosses). Although annual harmonics of amplitudes >1 Sv are evident in all but three years of data (Fig. 3b), the 1980–2007 mean properties, which to first-order represent the mean seasonal

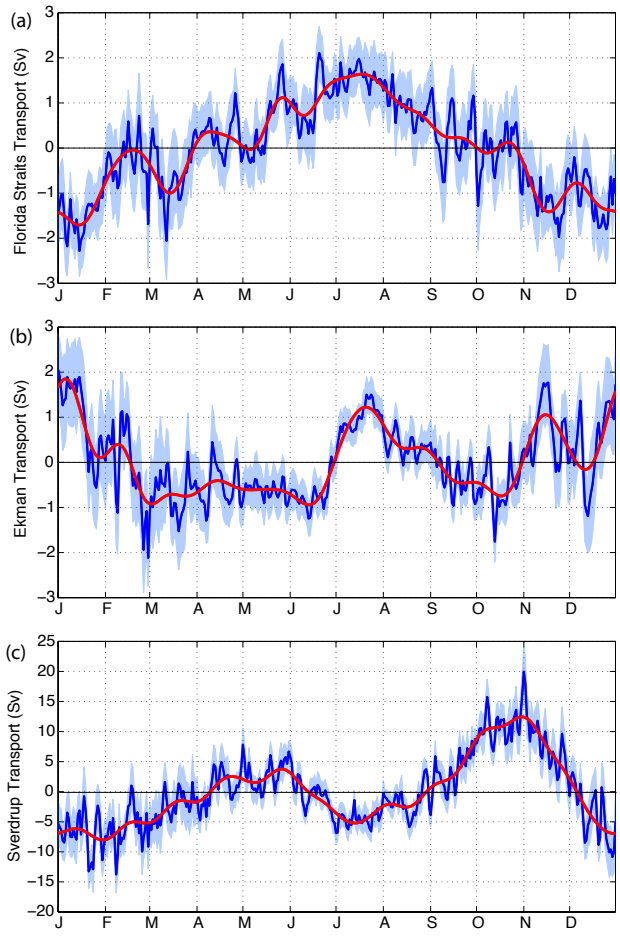

Fig. 2. Seasonal transport anomalies of **(a)** Florida Straits transport, **(b)** Ekman transport (26° N), **(c)** Sverdrup transport (26° N) for 1980–2007. Blue = daily means ± 1 standard error, red = 30-day low-pass on daily means.

cycle, only emerge when considering the full decadal length dataset. Harmonic coefficients (including confidence intervals) for the 1980–2007 mean seasonal cycle are given in Table 1.

Baringer and Larsen (2001) used 1982–1998 daily Florida Straits cable transports to identify an apparent change in the Florida Straits seasonal cycle when comparing the first and last 8-years of data (see also Fig. 4a). Figure 4 extends this analysis using monthly cable transports (calculated from daily transport data following DiNezio et al., 2009) to include the 8-year period 2000–2007. The 2000–2007 mean seasonal cycle is different in structure to both the 1982–1989 and 1990–1997 mean seasonal cycles (Fig. 4b–c) suggesting further changes in the seasonal cycle of the Florida Straits may have occurred. When including 95% confidence intervals on the estimates of monthly mean however (taking into account small sample size), it is not clear how significant these apparent changes in seasonal cycle actually are.

Table 1. Harmonic analysis for seasonal cycles of Florida Straits (1982–2007), Ekman (1980–2007, 26° N) and Sverdrup (1980–2007, 26° N) daily transports. Harmonic coefficients A-E represent least squares fit between data and the model: $A + B\cos(2\pi t/366) + C\sin(2\pi t/366) + D\cos(2\pi t/183) + E\sin(2\pi t/183)$, where t = time (days). Results are mean ± std. error of the coefficients calculated for each individual year of data (e.g. B_{Ekman} = mean of $B_{1980} + B_{1981} \ldots + B_{2007}$). Phase ($\phi$) and amplitude ($M$) are also given for annual/semi-annual harmonic constituents (model = $A + M_{an}\cos(2\pi t/366 - 2\pi\phi_{an}/366) + M_{\text{semian}}\cos(2\pi t/183 - 2\pi\phi_{\text{semian}}/183)$.

Coefficient	Florida Straits	Ekman 26° N	Sverdrup 26° N
A	32.07 ± 0.22	3.63 ± 0.11	-20.26 ± 0.37
B	-1.17 ± 0.27	0.26 ± 0.14	-0.73 ± 0.51
C	-0.01 ± 0.31	-0.34 ± 0.14	-3.71 ± 0.49
D	0.03 ± 0.26	0.58 ± 0.15	-4.38 ± 0.48
E	0.19 ± 0.22	0.22 ± 0.16	-4.63 ± 0.54
Phase	183/42 days	−53/11 days	−103/−68 days
Amplitude	1.17 0.19 Sv	0.43/0.62 Sv	3.78/6.37 Sv

To establish whether these changes are statistically significant, a Student's t-test was carried out for each pair of monthly mean transport estimates from each 8-year period (e.g. January mean 1982–1989 versus January mean 1990–1997), to test the hypothesis that the two values are statistically different. The confidence (p-value) in this hypothesis for each pair of values is shown in Fig. 4d–f. At 95% confidence, only the 1982–1989 August mean is different from the 1990–1997 mean (though high statistical confidence is also seen for August of 1982–1989 versus 2000–2007). This however appears due to the anomalously small confidence interval associated with the August 1982–1989 value. Nevertheless, the large July to November range associated with the somewhat asymmetric 1982–1989 seasonal cycle does produce high confidence values in both July-August and October-November (Fig. 4d) suggesting that it is possible that some change in seasonal cycle over time occurred. This is reinforced by Fig. 3b which shows the annual harmonics for the 1982–1989 period (black crosses) are more tightly clustered than the latter 8-year periods which become more scattered. A visual inspection of the monthly Florida Straits timeseries also reveals more distinct annual periodicity over this period relative to 1990 onwards (Fig. 1). No statistically compelling change is seen for further changes in seasonal cycle between 1990–1997 and 2000–2007 (Fig. 4f).

3.1.2 Relation of the seasonal cycle to seasonal winds at the western Atlantic margin

Whilst changes in the Florida Straits seasonal cycle remain plausible (particularly when comparing the mean seasonal cycle for 1982–1989 to more recent 8-year periods), significant transport variance at non-annual frequencies means

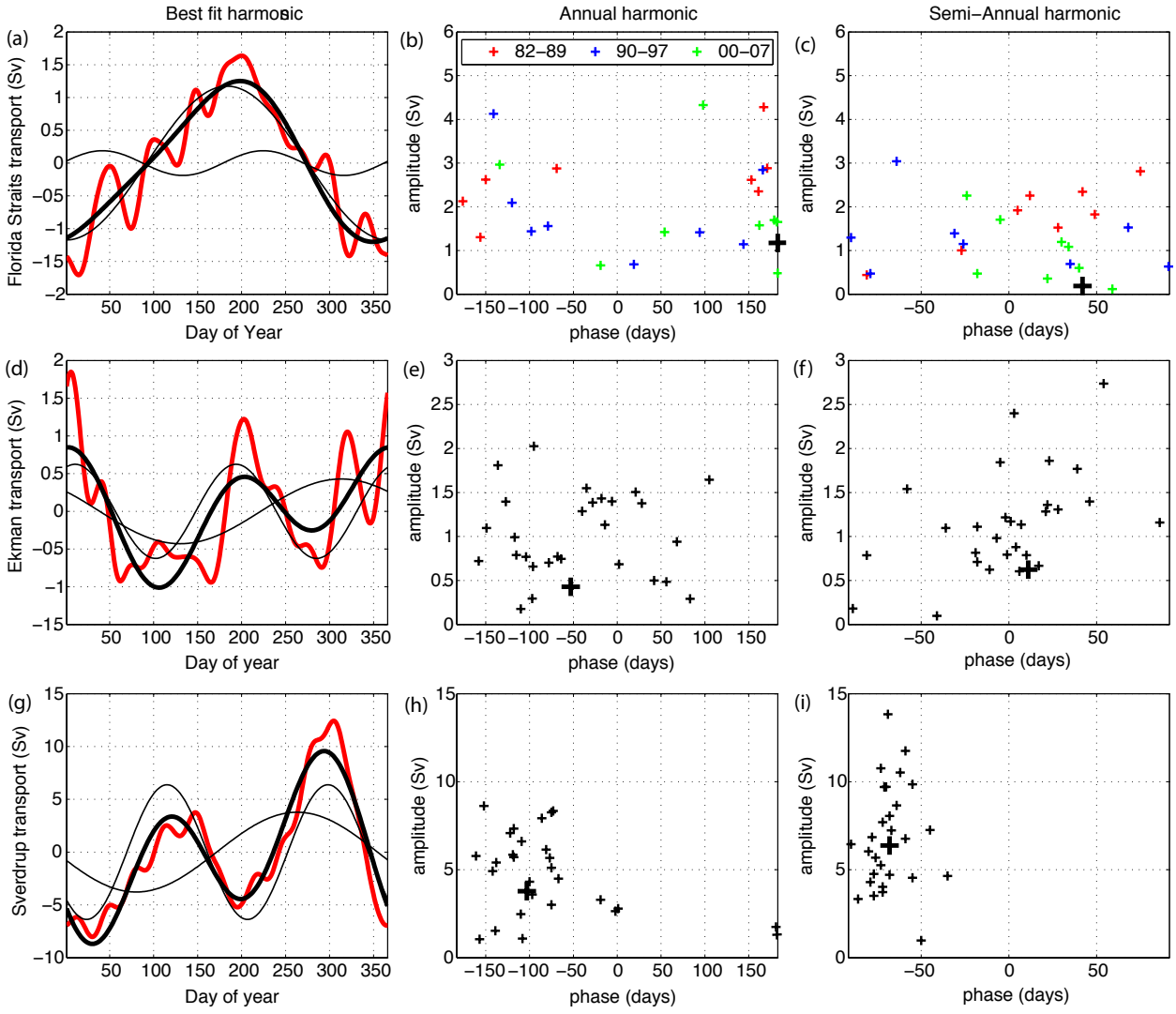

Fig. 3. **(a)** Annual and semi-annual harmonics (fine black lines) calculated for the Florida Straits 1982–2007 mean seasonal cycle (red, see also Fig. 2a). The bold black line shows the annual and semi-annual harmonics combined. **(b)** phases (ϕ) and amplitudes (M) of the annual harmonic (H_{an}) calculated for each year of Florida Straits data from 1980–2007; where $H_{an} = M\cos(2\pi t/\omega - 2\pi\phi/\omega)$ and t = time (days), ω=harmonic period (366 days). Red, blue and green crosses highlight harmonics for the 8-year periods; 1982–1989, 1990–1997 and 2000–2007 respectively. The bold black cross corresponds to the annual harmonic of the mean seasonal cycle shown in (a). **(c)** same as (b) but for the semi-annual harmonic (ω=183 days). **(d–f)**; same as (a–c) but for Ekman transport at 26° N (1980–2007). **(g–i)**; same as (a–c) but for Sverdrup transport at 26° N (1980–2007). Note that for Ekman and Sverdrup transports, black crosses are used to denote all harmonics from 1980–2007.

calculations of the seasonal cycle are liable to contamination by other signals (Fig. 5a). In the absence of a plausible physical mechanism it is difficult to be convinced of the significance of apparent changes in seasonal cycle. Several authors have attributed the Florida Straits seasonal cycle to wind stress forcing in the vicinity of the Florida Straits (Schott and Zantopp, 1985; Anderson and Corry, 1985a; Schott et al., 1988; Lee and Williams, 1988; Boning et al., 1991; Fanning et al., 1994) which shows similar seasonal phase to that of the Florida Straits transports. This is linked to the Florida Straits seasonal cycle through upstream wave propagation and local channel processes (e.g. Anderson and Corry, 1985a; Lee and Williams, 1988). Investigating this further using the NCEP-NCAR, NOC v1.1 and QuikSCAT climatologies, meridional wind stress both local to and downstream of the Florida Straits is also found to have seasonal phase comparable to the full 1982–2007 Florida Straits seasonal cycle (Fig. 6). It is notable that the seasonal cycle of

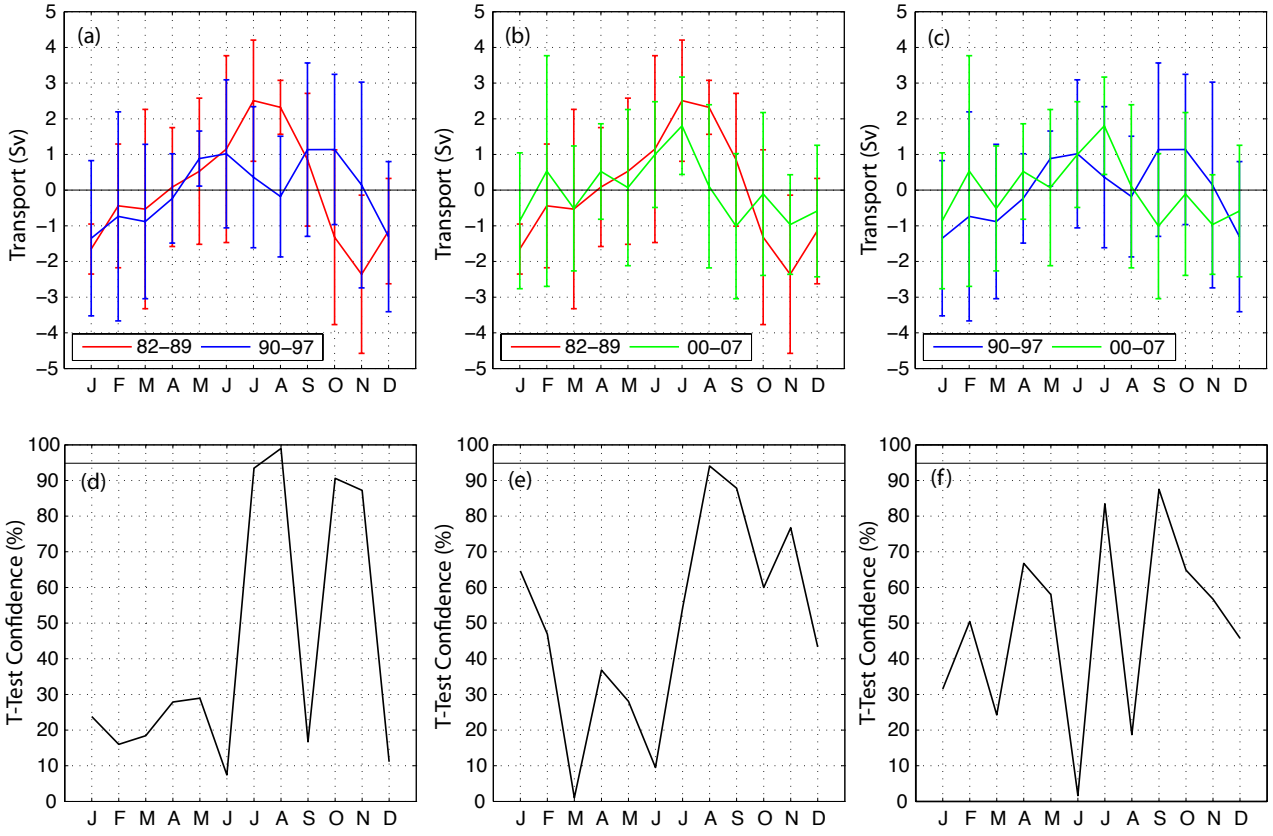

Fig. 4. **(a–c)** A comparison of Florida Straits seasonal cycle calculated over the 8-year periods 1982–1989 (red), 1990–1997 (blue) and 2000–2007 (green) using a timeseries of monthly Florida Straits transport. Error bars denote 95% confidence intervals associated with each monthly value. Mean transports for 1982–1989, 1990–1997, 2000–2007 and 1982–2007 are 32.4 Sv, 31.7 Sv, 32.1 Sv and 32.1 Sv respectively. **(d–f)** Results from a Student's t-test testing the hypothesis that monthly means from two separate 8-year periods are statistically different. Confidence in this hypothesis for each monthly pair in (a–c) is shown (the horizontal line corresponds to 95% confidence).

meridional wind stress downstream of the Florida Straits is larger in amplitude (and possesses more obvious annual periodicity) than in the Florida Straits itself and therefore may be most important in setting the Florida Straits seasonal transport cycle.

To establish whether changes in seasonal wind stress can explain apparent changes in Florida Straits seasonal cycle, seasonal wind stress was calculated over identical 8-yr periods to those used in Fig. 4 in regions upstream, downstream and local to the Florida Straits (Fig. 6, top left). In addition to meridional wind stress, seasonal cycles of zonal wind stress and wind stress curl were also calculated following work by Anderson and Corry (1985a) and Fanning et al. (1994) showing that the barotropic component of the Florida Straits seasonal cycle may be composed of contributions from all three wind stress parameters (both wind stress curl and the interaction of zonal/merdional wind stress with meridional/zonal topographic gradients). Whilst most literature links the Florida Straits seasonal cycle to local or downstream wind stress forcing, calculations for the region upstream of Florida Straits are also included following earlier work noting that wind stress curl over the Caribbean Sea also possesses similar seasonal phase to that of the Florida Straits transport (Schott and Zantopp, 1985; Schott et al., 1988). No evidence of this is seen however in the NCEP-NCAR, NOC v1.1 and QuikSCAT climatologies (Fig. 6, bottom right) so this region will be largely ignored in the following discussions. It is noted that the choice of regions shown in Fig. 6 is somewhat arbitrary, designed to overlap with previous literature, however the results shown are relatively insensitive to small changes in area. It is also noted that the three wind stress climatologies used are in excellent agreement for seasonal wind stress properties over these three regions, with only curl in region 1 showing any major discrepancies. However, as changes in wind stress curl remain qualitatively similar in region 1, this does not impact on later discussions.

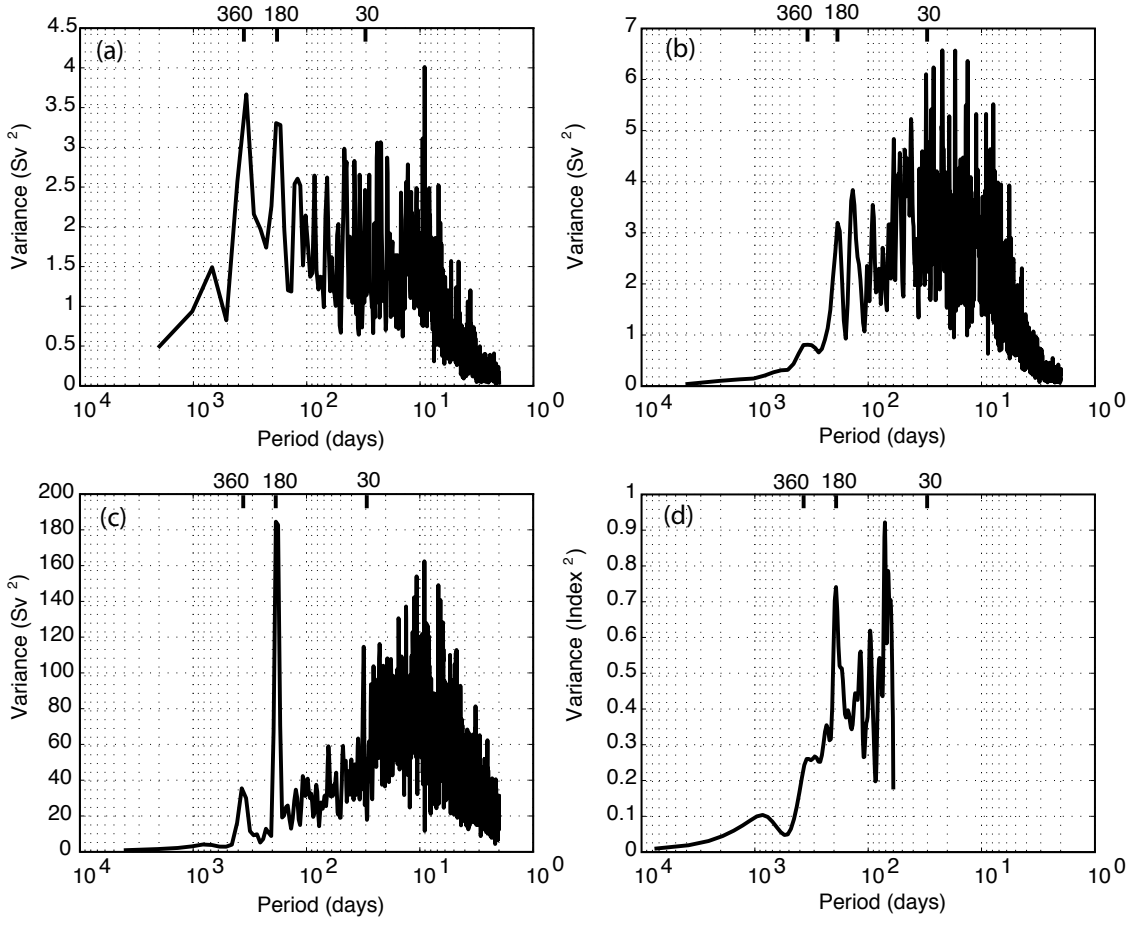

Fig. 5. Variance conserving spectra of **(a)** Florida Straits transport, **(b)** Ekman transport (26° N), **(c)** Sverdrup transport (26° N), **(d)** NAO index (monthly).

Over 8-year periods, seasonal wind stress in the vicinity of the Florida Straits appears very stable. No convincing evidence of relative changes in seasonal wind stress comparable to those seen in the Florida Straits transports is observed for any of the wind stress components investigated. For example, the 1982–1989 seasonal cycle of meridional wind stress downstream of Florida Straits (Fig. 6, centre row left) does not show a larger amplitude or greater asymmetry relative to 1990–1997 and 2000–2007, which is the case for transports in the Florida Straits (Fig. 4a–b). Given the marginal statistical significance of apparent changes in the Florida Straits seasonal transport cycle over 8-year periods and the absence of a wind-stress mechanism to drive them, it is therefore suggested that the changes observed in Fig. 4a–c are the result of transport variability at non-annual frequencies when calculating seasonal means (particularly periods <2 years where most of the transport variance occurs). The seasonal cycle of the Florida Straits is a property that emerges from a noisy signal when observations over decadal or longer periods are available.

3.1.3 Transport at non-seasonal timescales

The Florida Straits transport timeseries shows significant power at most periods >5 days (Fig. 5a) with discernible peaks at annual and semi-annual frequencies. Approximately 50% of the variance exists at periods longer than 60 days and around one third of the variance lies in the period band 60–720 days (std. dev. of 1.9 Sv) excluding the seasonal cycle (std dev. 0.8 Sv). The power spectra is nearly continuous indicating the Florida Straits transport is driven by randomly timed events. To understand Florida Current variability further it is therefore necessary to unpick changes in transport in a variety of different frequency bands.

At timescales of <5–10 days, Florida Straits transport variability shows coherence with along channel wind stress from both NCEP-NCAR and QuikSCAT climatologies, which in turn show greatest power at these high frequencies (Fig. 7a–c). This is in agreement with previous studies using different climatological winds (Johns and Schott, 1987; Schott et al., 1988; Lee and Williams, 1988;

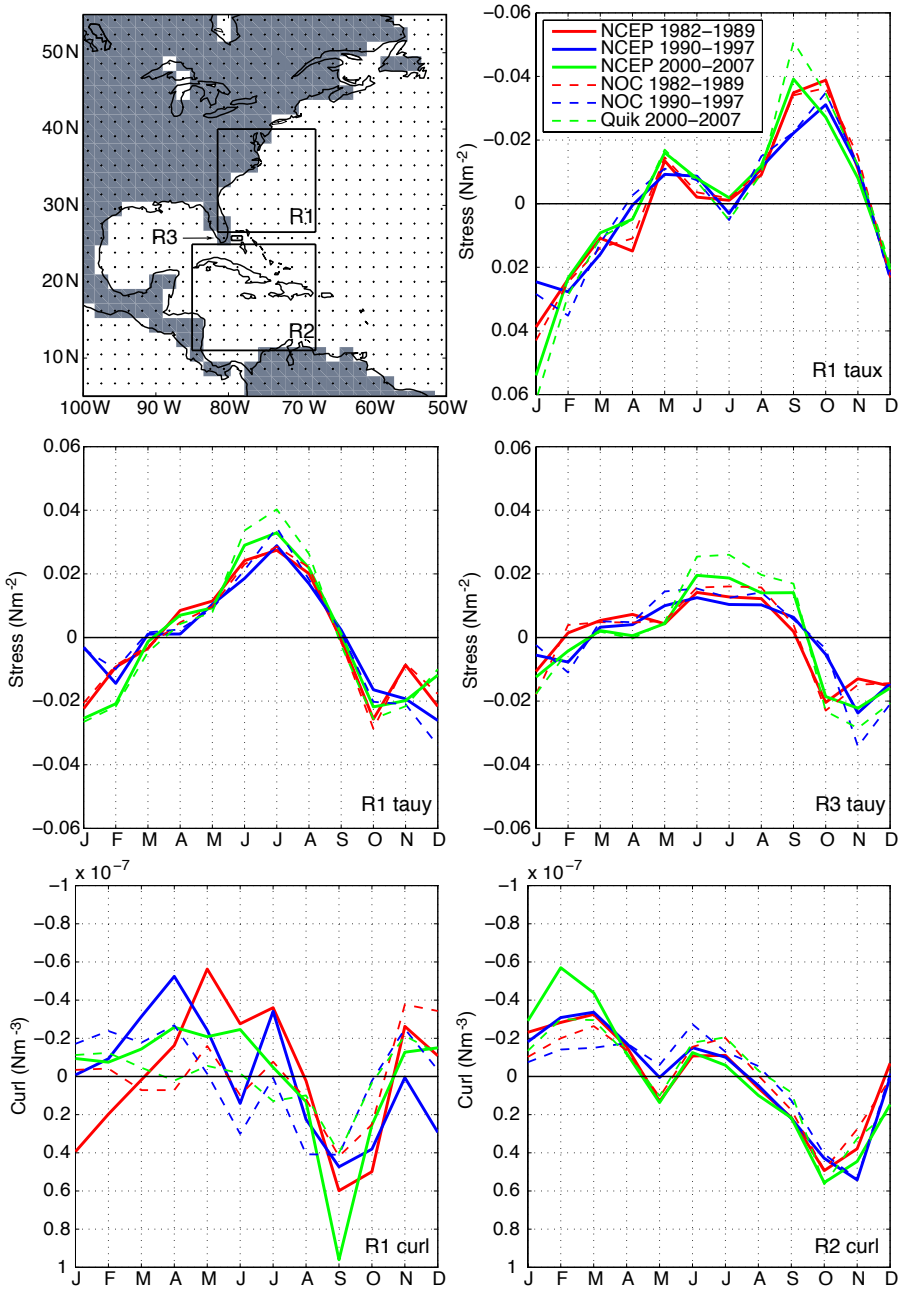

Fig. 6. Seasonal cycles of monthly wind stress parameters over the 8-year periods 1982–1989 (red), 1990–1997 (blue) and 2000–2007 (green) in 3 separate regions (R1-R3, see panel top left). Seasonal cycles are shown for the NCEP (solid lines) and NOC or QuikSCAT (dashed lines) climatologies where available. Note that y-axis orientation does vary to facilitate visual comparison with the Florida Straits seasonal transport cycle. Region of interest and wind stress parameter are stated in each panel (bottom right corner). Top left panel: Regions R1-R3 correspond respectively to regions downstream, upstream and local to the Florida Straits. Dots and shaded boxes denote the NCEP grid and land mask used in this study.

Greatbatch et al., 1995). The Florida Straits transport timeseries shows greatest power at sub-annual periods >10 days. Using a monthly timeseries of Florida Straits transport variability, various techniques were employed including cross-covariance, composite and Empirical Orthogonal Function (EOF) analysis, to identify possible links with the North Atlantic wind field at longer periods between 60–720 days (excluding the seasonal cycle). Despite extensive analysis, no clear relationships could be found with surface wind stress (meridional, zonal and curl) either local or remote to the

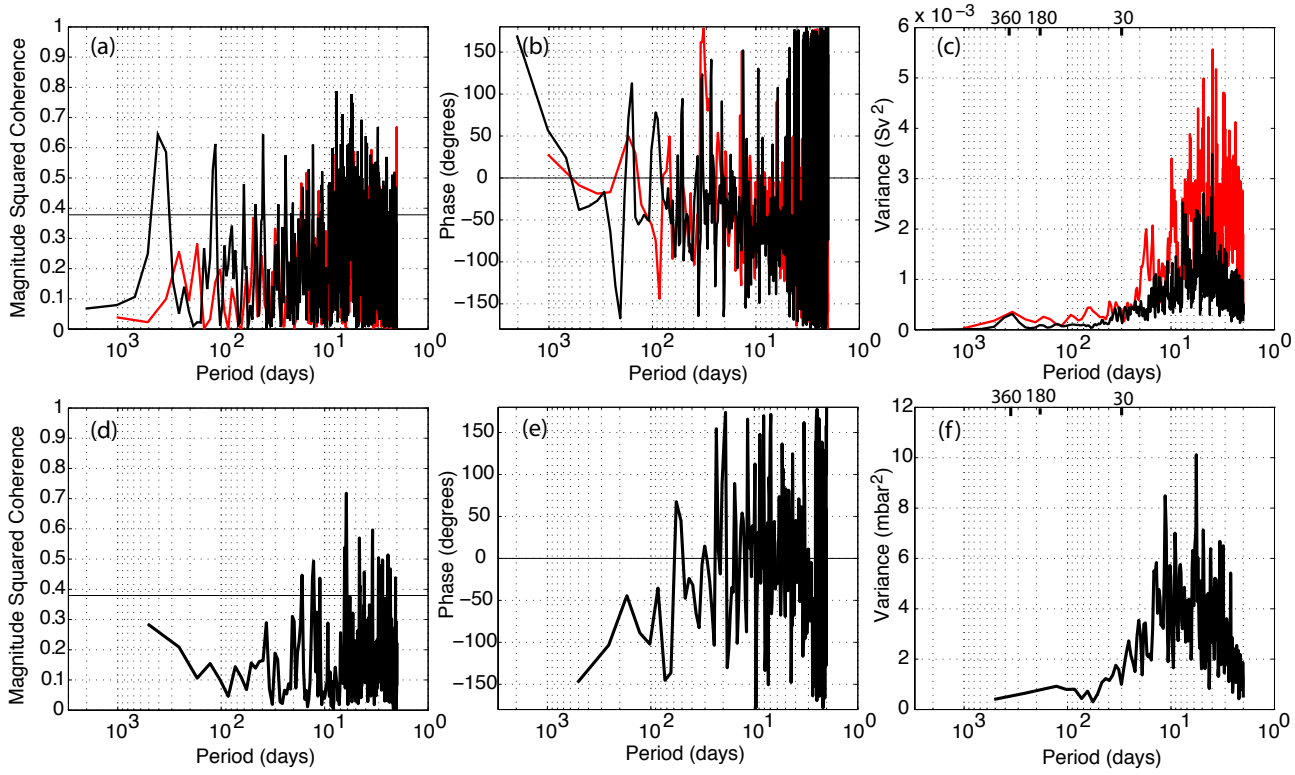

Fig. 7. (a) Coherence of Florida Straits transport with local meridional wind stress: black = NCEP wind at 27.62° N, 78.75° W from 1982–1998; red = QuikSCAT wind at 26.25° N, 79.25° W from 2000–2007. Horizontal line denotes 95% confidence level. **(b)** Phase corresponding to (a) (negative phase denotes wind leads). **(c)** Variance conserving power spectra for local meridional wind stress used in (a). **(d–f)** same as (a–c) replacing wind with NCEP sea level pressure gradient (between 27.62° N, 78.75° W and 33.33° N, 75° W) from 2002–2007.

Florida Straits. Particular attention was given to wind stress downstream of the Florida Straits which is potentially important for Florida Straits transport variability through coastal wave processes and barotropic signal propagation following f/h contours (Anderson and Corry, 1985a,b), however no significant relationships were found.

As expected from the lack of coherence with the North Atlantic wind field, a cross-correlation analysis between Florida Straits transport variability at periods between 60–720 days (1982–1998) and the NAO index shows no values of r exceeding 0.2 at lags up to 24 months. In addition, EOF analysis of surface wind stress variability surrounding the Florida Straits (20° N–40° N, 85° W–60° W) shows that PCs 1-4 possess little correlation with the NAO index (except PC1 of zonal wind stress where $r \approx 0.4$) and therefore it is regional modes of variability that are most likely to influence seasonal Florida Straits variability. This is consistent with regression maps of wind stress on the NAO index which indicate that in the western sub-tropical Atlantic the NAO only projects significantly on zonal wind stress (though peak zonal regression values are observed in the central Atlantic). Downstream of Florida Straits it is wind stress curl and the interaction of meridional wind stress with zonal topographic gradients and the North American coastline that might be expected to produce most response in the Florida Straits (Anderson and Corry, 1985b). It should be noted that at periods >2 years, reasonable correlation is seen between Florida Straits transport variability and the NAO (1982–1998) with the NAO index leading by ≈20 months (Baringer and Larsen, 2001), although since 2000 this relationship has become less clear (Beal et al., 2008). A possible explanation related to planetary wave propagation forced by wind stress curl in the open ocean has been identified by DiNezio et al. (2009).

The above analysis was repeated using NCEP-NCAR, NOC v1.1 and QuikSCAT climatologies whose wind stress variability shows a wide range of spatial correlation in the sub-tropical western Atlantic (particularly wind stress curl and meridional wind stress). Results were consistent between climatologies and no relationships with Florida Straits transport variability were found. Florida Straits transport variability at periods between 60–720 days (excluding the annual cycle) therefore seems difficult to interpret in terms of North Atlantic wind stress forcing.

The hypothesis was tested that Florida Straits variability is driven locally by changes in Sea Level Pressure (SLP) which act to pump water in and out of the Straits. No clear

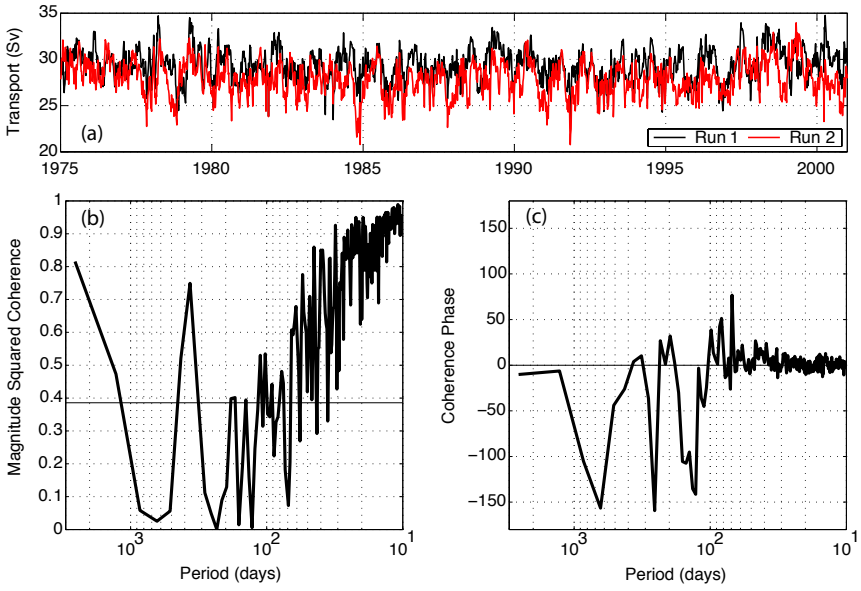

Fig. 8. (a) Transport through the Florida Straits for two 1/4° NEMO passes with identical external ocean forcing but differing initial ocean state, **(b)** coherence (horizontal line denotes 95% confidence level) and **(c)** phase for the two ocean model passes.

coherence is seen however between gradients in NCEP SLP (the difference between local SLP and SLP at various locations several hundred kilometers outside the Florida Straits) and Florida Current transport variability, providing little evidence for this mechanism (Fig. 7d–f). This is in agreement with the barotropic model study of Greatbatch et al. (1995) which showed negligible contribution of atmospheric pressure forcing to Florida Straits transport variability at periods >2 days due to an approximately isostatic ocean response.

3.1.4 The influence of internal ocean transport variability

To understand the importance of internal ocean variability in the Florida Straits transport measurements, a single NEMO run comprising of two passes of the DFS 3 forcing dataset (ORCA025-N102 and ORCA025-N112), undertaken at the National Oceanography Centre, Southampton as part of the DRAKKAR suite of eddy-permitting 1/4° NEMO model runs (Barnier et al., 2006; Madec et al., 2008; Grist et al., 2010), was used opportunistically to estimate transport variance associated with this process. Each pass covers the period 1958–2001 and is forced using identical external ocean fluxes (momentum and buoyancy) with output available at 5-day resolution. The model starts from rest, with a climatological state. The final ocean and ice state from pass 1 (N102) is used to initialise the start of pass 2 (N112), facilitating studies of climatic drift in the model. For the purposes of this study, these two passes also allow the behaviour of two model oceans with differing initial states but identical surface fluxes to be compared.

The 1/4° NEMO model possesses realistic bathymetry which includes a Florida Straits channel separated from the ocean interior by Bahamian islands. Time series of Florida Straits transport were extracted from each model pass and compared over the period 1975–2001 (where drift effects in pass 1 were no longer evident). The simulated Florida Straits transports are shown in Fig. 8a. Mean transport for the two passes is 29.3 Sv and 27.9 Sv which compares favorably with the observed Florida Straits mean transport of 32.1 Sv. The phase and amplitude of model and observed seasonal cycles are also very similar though model variability is somewhat damped at most frequencies (the std. devs. of pass 1, pass 2 and observations are 1.7 Sv, 1.8 Sv and 3.2 Sv respectively).

Passes 1 and 2 show a correlation of $r = 0.56$. The standard deviation of the difference between the two passes is 1.69 Sv with most power at periods of 70–1000 days. This is emphasised in Fig. 8b–c where little significant coherence is seen between the two passes over this period range (except notably at seasonal periods) and the zero phase relationship breaks down. The power spectra of the difference between the passes is mostly composed of oceanic variability at a range of frequencies in the ≈70–1000 day band. No obvious peaks are found in the spectra that may suggest unrealistic ringing generated by coherent basin modes.

Given identical external forcing of the two model passes, any loss of coherence can be attributed to internal oceanic variability i.e. variability that is not directly forced by changes in winds and surface buoyancy fluxes. A significant drop in coherence at intra-seasonal to interannual periods is characteristic of oceanic eddy and wave variability at subtropical latitudes and suggests that these processes make a

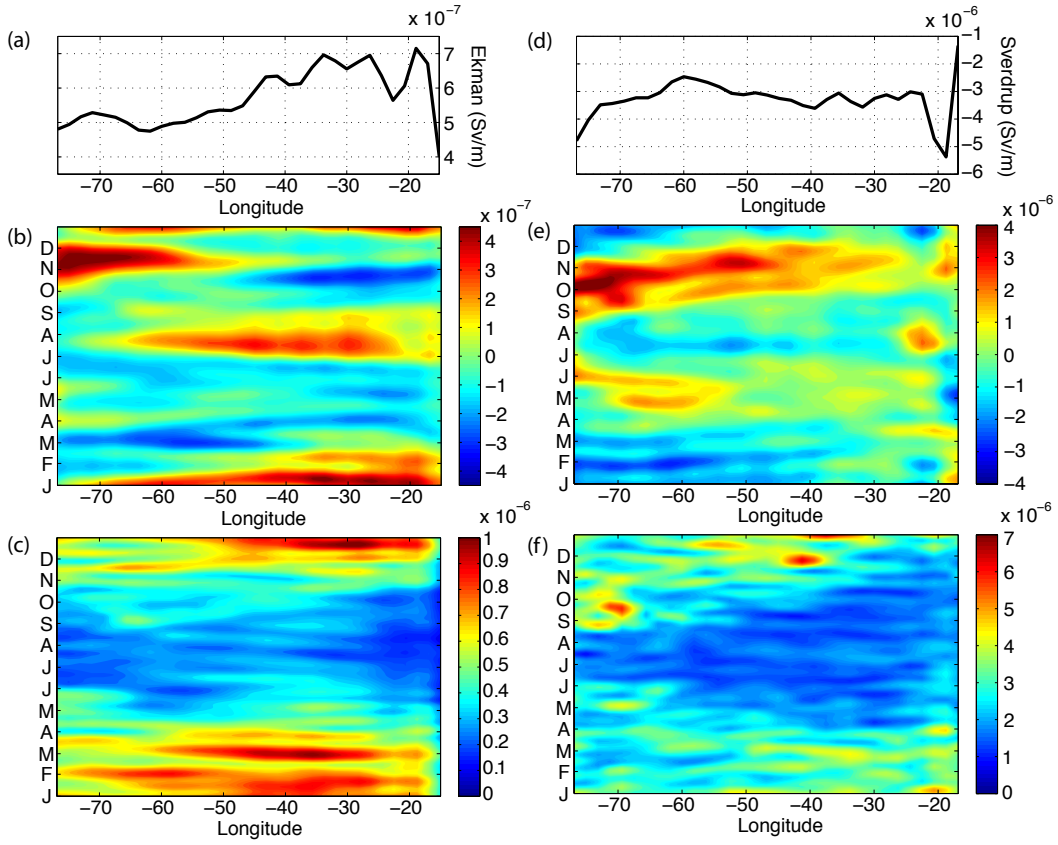

Fig. 9. Ekman **(a–c)** and Sverdrup **(d–f)** transports from 77–15° W and 77–16.9° W respectively at 26° N. (top row) mean transport, (middle row) seasonal cycle (mean transport removed), (bottom row), seasonal variance (1 Std. Dev.). All transports are given in Sv m^{-1} (Eqs. 1 and 2, RHS $\div L_x$). Mean Ekman and Sverdrup transports at 26° N are 5.7×10^{-7} Sv m^{-1} and -3.3×10^{-6} Sv m^{-1} respectively.

substantial contribution to Florida Straits variability at these periods. This may well explain the lack of correlation seen between observed Florida Straits transport variability and monthly North Atlantic wind stress at 60–720 periods (excluding the annual cycle) described in Sect. 3.1.3. It is noted that the internal ocean contribution to Florida Straits transport variability is likely to be underestimated as eddy activity in eddy-permitting models tends to be more predictable than in eddy resolving models.

The significant coherence seen at annual period in Fig. 8b-c support the view that the annual Florida Straits transport cycle is driven by the annual cycle of regional wind stress (as discussed in the preceding sections). Large coherence at periods >1000 days is perhaps also unsurprising as at multi-annual or longer periods, western boundary current variability at 26° N is expected to reflect changes in sub-tropical gyre and thermohaline circulation, responding to changes in wind stress curl and high latitude buoyancy forcing respectively. Although some Florida Straits transport coherence with local meridional winds stress was identified at periods <10 days (Fig. 7a–b), the important role of external ocean forcing at 10–70 day (and perhaps ≈ 100 day) periods, highlighted by significant coherence in this band (Fig. 8b), remains unexplained.

3.2 NCEP Ekman transports

The seasonal cycle of northward Ekman transport across 26° N is shown in Fig. 2b. Transport (bold red line) reaches a maximum of +1.8 Sv and +1.2 Sv in mid-January and mid-July and a minimum of −0.9 Sv in early March and mid-June. No clear annual periodicity is observed in the seasonal cycle of Ekman transport at 26° N, which is further complicated by a secondary maxima in mid-November (1 Sv) and a secondary minima in mid-October (−0.7 Sv). The Ekman transport seasonal cycle shown in Fig. 2b can be partially understood as the sum of two somewhat distinct seasonal transport regimes east and west of ≈50–60° W (Fig. 9b). East of 50–60° W, Ekman transport shows a pronounced semi-annual cycle with maximum northward transport in January and July and minimum northward transport in March-June and October. West of 50–60° W, Ekman transport shows something of an annual cycle with maximum northward

transport in November and minimum northward transport from February to June.

Figure 10 shows wind stress at 26° N in a wider North Atlantic context. Transport maxima in January and July are associated with atmospheric circulation around low and high SLP centres in the central tropical and mid-latitude Atlantic respectively. These act to enhance the mean zonal wind stress at 26° N associated with the westward trade winds (Fig. 9a). Transport maxima in November are associated with strong southwesterly wind stress in the western sub-tropical Atlantic driven by strong SLP gradients between a high pressure over North America and a low pressure in the central Atlantic near 26° N. At 26° N, the reduced section-wide coherence of Atlantic zonal wind stress contributes to a complex seasonal cycle in comparison with latitudes outside the sub-tropics (Fig. 10). Seasonal wind stress anomalies are generally much larger away from the sub-tropical latitudes.

Following the harmonic analysis of the Florida Straits transport, Fig. 3d shows annual and semi-annual harmonic components fitted to the Ekman seasonal cycle at 26° N. The combination of these two harmonics only partly captures the structure of the observed seasonal cycle (rms error =0.5 Sv), possessing amplitudes of 0.43 Sv and 0.62 Sv respectively (Table 1). Seasonal cycle features such as the abrupt January, July and November northward transport maximums are not well resolved by these low-order harmonics. Figure 3e-f shows the interannual variability of the phase and amplitude of the annual and semi-annual harmonic components for the period 1980–2007. Both harmonic components show significant interannual variability demonstrating that, similar to the Florida Straits transport, the Ekman transport seasonal cycle is a property that only emerges from decadal observations of a noisy signal. Estimates (including standard errors) of the annual and semi-annual coefficients that describe in part the Ekman transport seasonal cycle at 26° N are given in Table 1. Ekman transport at 26° N shows only modest power at semi-annual and annual periods with significant power observed across a broad range of frequencies, particularly in the 5–60 day band (Fig. 5b). In contrast with the seasonal cycle, this variability shows section-wide coherence at 26° N, reaching a maximum in Winter and early Spring (Fig. 9c).

A significant source of Ekman transport variability at 26° N is the NAO. The correlation between monthly Ekman transports across 26° N and the NAO index is $r = 0.55$, as previously noted by Josey et al. (2002). Correlation with the NAO index is similar at sub-annual and interannual and longer timescales ($r \approx 0.5$) and significant coherence is seen at various periods ranging from seasonal to decadal (Fig. 11a–b). NAO driven Ekman transport variability is in phase section-wide at 26° N but with enhanced variance in the central and eastern basin which is closer to the NAO Azores pressure centre. EOF analysis reveals a similar section-wide mode of variability accounts for ≈ 60% of both sub-annual and interannual Ekman transport variability at 26° N, though only moderate correlation between PC1 and the NAO index ($r \approx 0.5$) suggests this is in part attributable to Azores high variability unrelated to the NAO. No obvious relationship with other major modes of Northern Hemisphere atmospheric circulation is seen in the Ekman transport signal at 26° N. Enhanced section-wide variability, seen from December to March in Fig. 9c, can be partially attributed to the NAO which is at it's strongest in boreal Winter.

Regression of Ekman transports integrated across 26° N on the NAO index results in a change of ≈ +1 Sv per NAO index unit (note that this will be greater in Winter as the NAO index used is effectively normalised such that index variability is not enhanced in Winter). During positive NAO conditions, a strengthening of the Azores high enhances the mean easterly wind stress resulting in increased northward Ekman transport. At multi-decadal timescales, the seasonal cycle shown in Fig. 2b may be somewhat biased given the positive mean state of the NAO over the period 1980–2007. Over the periods 1980–2007 and 1950–1979, the NAO index showed +0.1 and −0.1 mean state respectively. A comparison with the seasonal Ekman transport cycle for the period 1950–1979 shows that January-March mean northward transport is enhanced by 1.3 Sv in 1980–2007 relative to 1950–1979 (whilst year-round mean northward transport is increased by 0.2 Sv). This accounts for the January-March seasonal cycle peak seen in Fig. 2b which is not apparent during 1950–1979.

3.3 NCEP Sverdrup transports

The seasonal cycle of Sverdrup transport across 26° N is shown in Fig. 2c. Transport (bold red line) reaches a maximum of +12.4 Sv in early November and a minimum of −8.0 Sv in early February. A semi-annual periodicity is observed in the seasonal cycle of Sverdrup transport at 26° N (secondary maxima and minima of + 3.8 Sv and −5.2 Sv are observed in late May and mid-July respectively), though with an asymmetry resulting from significantly weakened southward transport in late Autumn. The range and structure of the seasonal cycle is similar to that previously described for other wind stress data (e.g. Mayer and Weisberg, 1993). Figure 9e shows this semi-annual variability is present across most of the Atlantic at 26° N with greatest amplitude west of ≈40–50° W. Quite different seasonal (and mean; Fig. 9d) structure is seen however approaching the eastern basin margin east of ≈30° W which appears partially due to the seasonal heating and cooling of the West African land mass. The Autumn southward transport minimum occurs due to a combination of almost section-wide northward transport anomalies from September through November and strong regional cyclonic circulation around a SLP low that develops seasonally near 26° N in the central and western Atlantic (Fig. 10).

Similar to the analysis of Florida Straits and Ekman transports, annual and semi-annual harmonic components are fitted to the Sverdrup transport seasonal cycle at 26° N (Fig. 3g). The combination of these two harmonics captures

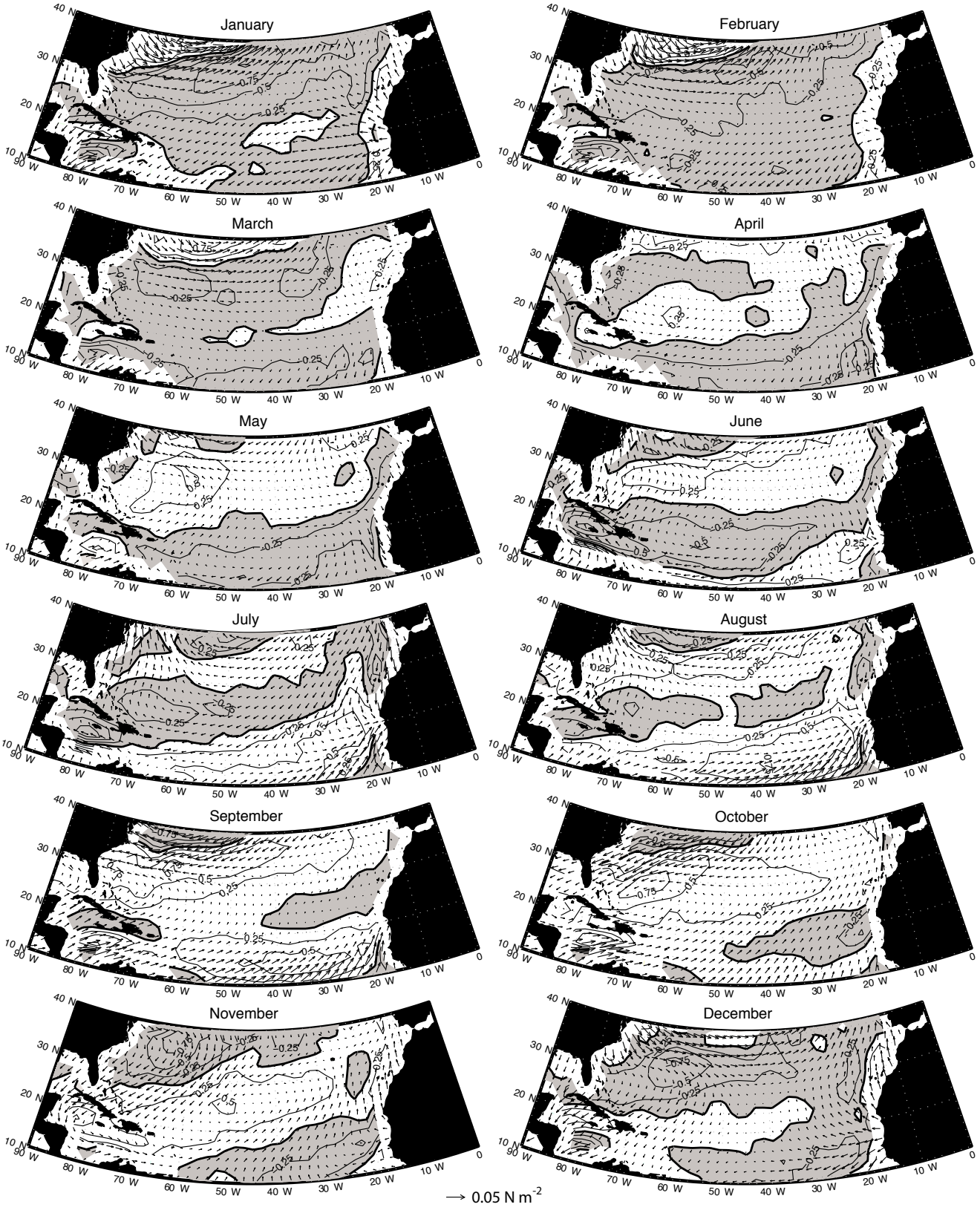

Fig. 10. The seasonal cycle of wind stress (vectors) and curl (contours; shaded patches denote negative curl) in the sub-tropical North Atlantic.

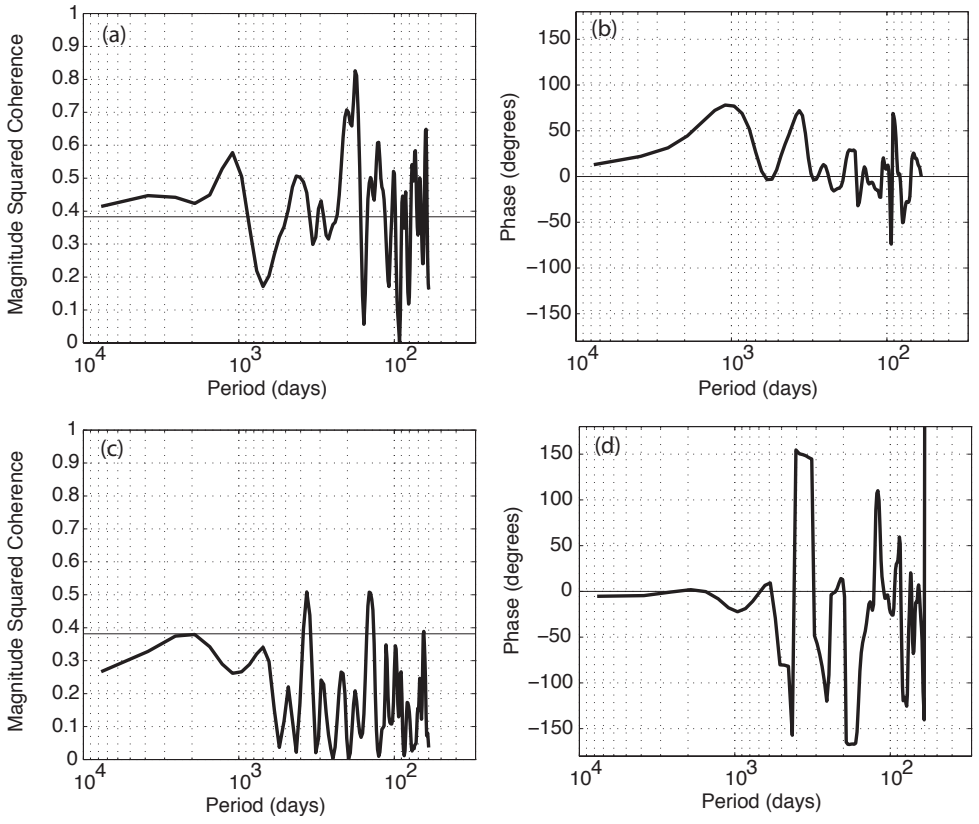

Fig. 11. (a) Coherence of Ekman transport at 26° N with monthly NAO index (1980–2007, horizontal line denotes 95% confidence level), **(b)** Phase corresponding to coherence in (a) (negative phase denotes NAO leads), **(c–d)** same as (a–b) but for Sverdrup transport at 26° N.

the observed seasonal variability (rms error = 1.6 Sv), although the amplitude of the semi-annual component is much greater (6.4 Sv, see Table 1). The interannual variability of the phase and amplitude of these harmonic components for the period 1980–2007 is shown in Fig. 3h–i. The semi-annual harmonic shows only small interannual phase variability with more pronounced variability in amplitude whilst the annual harmonic is also quite stable but shows greater variability in phase which acts to modify the semi-annual asymmetry seen for the mean seasonal cycle (Fig. 2c). Seasonal Sverdrup transports at 26° N are therefore more stable from year to year than either the Ekman or Florida Straits transports, though with some modulation in amplitude. Annual and semi-annual harmonic coefficients (including standard error) are given in Table 1.

The power spectra of Sverdrup transport across 26° N show greatest power at semi-annual period (Fig. 5c) along with a modest spectral peak at annual period. Significant power is observed at most sub-decadal frequencies, including a notable jump in power at periods $<\approx 40$ days. Across 26° N, variability (excluding the seasonal cycle) is enhanced section-wide from late Autumn to early Spring, though enhanced variability persists for longer in the western Atlantic (Fig. 9c) The source of Sverdrup transport variability across 26° N however is not clear and likely represents a combination of several modes of variability. Monthly Sverdrup transports across 26° N show no significant correlation with the NAO index and marginal coherence with the NAO is only seen across narrow frequency bands (Fig. 11c–d). Low pass filtered southward Sverdrup transports (36 month cut-off period) do show good correlation with the NAO index, particularly in the central and western Atlantic basin ($r = -0.64$, see also DiNezio et al., 2009). However significance is limited by a long integral timescale and relatively short time-series so coherence at longer timescales is not yet assumed (note that no strong correlation is observed over the period 1950–1979). An EOF analysis of sub-annual Sverdrup transport variability reveals no dominant modes exist. EOF's 1 and 2 have section-wide structure but account for $< 50\%$ of variance and show no clear correlation with any major mode of Northern Hemisphere atmospheric circulation. At interannual timescales, EOF1 (45% of variance) reveals variability is somewhat concentrated in the central and eastern Atlantic. Sub-decadal variability of the wind stress curl field at 26° N is less spatially coherent (more localised longitudinally and latitudinally) than for zonal wind stress (Ekman transports).

At decadal timescales, the seasonal cycle shown (Fig. 2c) does appear biased by the positive mean state of the NAO for the period 1980–2007. Comparison with the seasonal Sverdrup transport cycle for the period 1950–1979 (when the NAO index shows negative mean state) demonstrates January-March mean southward transport (when the NAO is strongest) is reduced by 3.6 Sv in 1980–2007 relative to 1950–1979. Annual mean southward transport is reduced by 1 Sv. Regression of Sverdrup transports across 26° N on the NAO index suggests that on decadal timescales a change of ≈4–5 Sv per NAO index unit may be expected i.e. a weakening of mean southward transport and the subtropical gyre in response to positive NAO state. This result should be approached with some caution. From 1980–2005 the NOC v1.1 climatology shows a negative Sverdrup transport trend of $-0.2\,\mathrm{Sv\,yr^{-1}}$ compared to a positive trend of $+0.1\,\mathrm{Sv\,yr^{-1}}$ for NCEP (Longworth, 2007, and this study) and therefore it is not clear how reliable such long term wind stress curl trends (and therefore long-term relationship with the NAO) may be.

3.4 Ekman and Sverdrup transports from NOC and QuikSCAT

Whilst Sects. 3.2–3.3 have concentrated on analysis of the NCEP-NCAR reanalysis climatology, a comparison of NCEP-NCAR Ekman and Sverdrup transports with the 1° NOC v1.1 climatology and 0.5° IFREMER MWF QuikSCAT climatology reveals good agreement in terms of zonally integrated properties across 26° N (note that the NCEP-NCAR reanalysis assimilates QuikSCAT data). Correlation of monthly NCEP-NCAR transport timeseries with those of NOC/QuikSCAT are 0.96/0.96 respectively for Ekman transports and 0.76/0.91 respectively for Sverdrup transports. Coherence is generally greatest at annual periods, reducing at both higher and lower frequencies, whilst power spectra for all three climatologies are similar in character. NCEP-NCAR power appears reduced at most frequencies relative to NOC and especially QuikSCAT, which is expected given that the coarser NCEP-NCAR grid limits its ability to resolve small scale variability. Considering transport as a function of longitude, all three climatologies are in reasonable agreement across most of 26° N (including analysis of the seasonal cycle) although the coherence between NCEP-NCAR and NOC Sverdrup transports reduces sharply east of ≈40° W. At the basin margins, coherence between climatologies dips markedly, especially in the lee of the Canary Islands where fine scale turbulence is not well resolved on the coarser grids of NCEP-NCAR and NOC (as previously noted by Risien and Chelton, 2008). Note that these discrepancies have little effect in terms of the zonally integrated properties presented in Sect. 3.2–3.3. A dip in coherence between climatologies is also seen over the Gulf Stream where the effects of strong SST gradients on surface wind stress are not well resolved by NCEP-NCAR and NOC (also noted by Risien and Chelton, 2008).

3.5 Error in the Florida Straits, Ekman and Sverdrup transport timeseries

Whilst this work has mostly followed a statistical approach, measurement errors are now briefly discussed. For the Florida Straits transport, errors in daily mean instantaneous (3-day low-pass filtered) measurements amount to 1.7 Sv rms with the errors predominantly random (Larsen, 1992; Meinen et al., 2010). The observed variability of daily Florida Straits transports is 3.3 Sv rms, thus random errors account for ≈25% of variance and the signal to noise ratio is substantial. Much of this study uses monthly mean Florida Straits transports, constructed from 15 or more daily values (following DiNezio et al., 2009) so random measurement error associated with monthly means is a maximum of ≈0.4 Sv rms ($1.7/\sqrt{15}$). The observed variability of monthly Florida Straits transport is 2.4 Sv rms, thus measurement errors account for ≈3% of variance and the signal to noise ratio is large.

For monthly Ekman and Sverdrup transports across 26° N, differences in mean transport between climatologies provide an estimate of bias whilst r^2 values and rms differences (between demeaned and detrended timeseries) provide an estimate of random error (because NCEP-NCAR assimilates QuikSCAT data, the two cannot be considered strictly independent). For Ekman transports, mean transports for 2000-2005 (where the NCEP-NCAR, NOC v1.1 and IFREMER MWF QuikSCAT climatologies overlap) have a range of 0.2 Sv, whilst r^2 values are > 0.9 (indicating over 90% of the timeseries variance is accounted for between climatologies) and rms differences range from 0.5-0.8 Sv (in comparison with NCEP Ekman transport variability of 1.9 Sv rms). Ekman transport variability across 26° N appears well defined relative to the differences (random errors) between climatologies. The mean bias estimated here is consistent with the more conservative estimate used by RAPID-WATCH of ± 0.5 Sv (Kanzow et al., 2010) accounting for uncertainties in wind measurements and drag coefficient. For Sverdrup transports, mean transports for 2000-2005 have a range of ≈3 Sv (though this is more a result of differing climatology trends), r^2 values range from ≈0.6–0.8 and rms differences range from 6.0–8.5 Sv (in comparison with NCEP Sverdrup transport variability of 8.0 Sv rms). Sverdrup transport variability across 26° N appears reasonably coherent between climatologies but care should be taken interpreting short sections of the record where differences (random errors) between climatologies may be comparable in magnitude to the signal of interest. This study only addresses Sverdrup transport properties derived from the full record.

4 Discussion

4.1 Comparison of Florida Straits, Ekman and Sverdrup transport seasonal cycles

The long-term mean seasonal transport anomalies of the Florida Straits, Ekman and Sverdrup transports at 26° N are presented in Fig. 2. All three seasonal cycles are both well defined and distinct from one another. The Florida Straits seasonal cycle has a dominantly annual periodicity whilst the seasonal cycle of Sverdrup transport has a clear semi-annual component (Table 1). Seasonal Ekman transport integrated across 26° N has no dominant annual nor semi-annual component. No obvious relationship exists between any of these three timeseries.

The large semi-annual amplitude of Sverdrup transports east of the Florida Straits is not matched by an equivalent anti-phased response in the Florida Straits, as predicted by simple Sverdrup dynamics. Instead, the Florida Straits has a semi-annual component of much smaller amplitude (though somewhat in anti-phase, Table 1) due to the blocking effect of the continental shelf and Bahamian islands (Anderson and Corry, 1985b). The same is true of the annual components of the Florida Straits and Sverdrup transports, which show no anti-phased relationship and a large difference in amplitude. This disagreement between the observed Florida Straits seasonal cycle and that predicted by Sverdrup dynamics has long been known (e.g. Schott and Zantopp, 1985). The seasonal cycle in Florida Straits transport is instead thought to be set chiefly by meridional wind stress local and downstream to the channel, a view supported by this study.

The general difference in appearance of Florida Straits, Ekman and Sverdrup transport seasonal cycles is a result of the contrasting structure of the meridional, zonal and curl wind stress fields near 26° N. In the western sub-tropical Atlantic, northward Summer wind stress reverses to southwestward wind stress in late Autumn (Fig. 10), driving both the Florida Straits annual cycle and strong northward regional Ekman transport in Autumn. In the central and eastern Atlantic at 26° N, Ekman transport is semi-annual in character, leading to an integrated basinwide seasonal transport of quite irregular character. Whilst Ekman and Sverdrup semi-annual components are nearly in anti-phase (i.e. westward wind stress appears associated with negative wind stress curl) the semi-annual component of wind stress curl is more in phase across the basin (except approaching the eastern boundary, Figs. 9e and 10) leading to a Sverdrup transport seasonal cycle with clear semi-annual periodicity.

4.2 Emergence of the Florida Straits seasonal transport cycle from a noisy signal

For the Florida Straits transport (1982–2007) a seasonal cycle possessing a clear annual period emerges from the observations. This is in contrast to earlier work that envisaged a more asymmetric seasonal structure (e.g. Schott and Zantopp, 1985; Leaman et al., 1987; Schott et al., 1988; Lee and Williams, 1988; Greatbatch and Goulding, 1989; Rosenfeld et al., 1989; Boning et al., 1991; Fanning et al., 1994) or the possible emergence of a semi-annual like structure in the 1990s (Baringer and Larsen, 2001). Whilst some asymmetry of the long-term seasonal cycle is revealed by harmonic analysis, this asymmetry is marginal and the Florida Straits seasonal transport cycle is dominated by its annual component (Table 1).

The Florida Straits transport timeseries at 26° N is very noisy relative to its seasonal cycle resulting in large year to year variability of the annual and semi-annual harmonic components about their long term means (Fig. 3a–f). In the case of such noisy data, there is a need for decadal length datasets when estimating even basic seasonal properties and caution should be exerted when calculating similar properties for other shorter timeseries. Apparent changes in the seasonal cycle of Florida Straits transports over 8-year periods provide an ideal case study of the hazards involved when estimating seasonal properties using relatively short datasets. Whilst Florida Straits seasonal transports constructed from monthly means appear quite different in structure when comparing 8-year periods, this is the result of contamination by variability at other frequencies while the underlying seasonal cycle is stable. This is in agreement with Meinen et al. (2010) who use a Monte Carlo style evaluation to conclude the 8-year changes in seasonal cycle are not statistically different from each other. The Ekman transport seasonal cycle at 26° N also only emerges from decadal length observations.

A caveat to the above discussion is acknowledged. The model decompositions of Anderson and Corry (1985a) and Fanning et al. (1994) show the Florida Straits seasonal transport cycle results from the combined effects of several regional wind stress parameters. Whilst no single wind stress parameter showed evidence of relative changes matching those seen in the Florida Straits over 8-year periods (suggesting the Florida Straits seasonal cycle has not changed over time, Sect. 3.1.2 and Fig. 6), subtle changes of several parameters cannot be as easily ruled out as a possible mechanism driving changes in the seasonal transport cycle. Further study of this issue may therefore be warranted.

The Florida Straits transport timeseries shows significant power at most periods >5 days and around a third of the variance lies in the period band 60–720 days. This band contributes significantly to the noise that obscures calculations of the seasonal cycle from short records and this study gives particular attention to defining its source. Variability at these timescales has received relatively little attention in the literature. An intensive study of the Florida Current made during the STACS program by a variety of measuring techniques had provided some information on the structure of variability in the Florida Straits (e.g. Molinari et al., 1985; Leaman et al., 1987; Schott et al., 1988), however the relatively short time scale of the STACS observations (a few years) made it

difficult to resolve variability on the sub-annual to interannual periods of interest here.

Good reason exists to believe that at 60–720 day timescales, Florida Straits transport variability may be related to local or regional wind stress. At sub-decadal timescales the continental shelf and Bahamian islands act to shield the Florida Straits from mid-oceanic wind stress variability (Anderson and Corry, 1985b). Mayer and Weisberg (1993) found significant coherence in the 182–393 day period band between sea level difference across the Florida Straits near 26.5° N (a proxy for Florida Current volume transport) and the shore-parallel wind stress component north of the straits (from the COADS dataset) for the period 1982–1988 and concluded that coastally trapped waves are important for the annual cycle of transport within the straits. In this study, no significant relationships were found at 60–720 day periods (excluding the seasonal cycle) between Florida Straits variability and local, regional or remote North Atlantic wind stress. In combination with results from a 1/4° eddy-permitting ocean model, this suggests that internal oceanic processes (e.g. mesoscale features) play an important role in variability at these periods.

A detailed investigation of this internal ocean variability is beyond the scope of this study, however possible sources can be discussed. The magnitude of Florida Straits transport variability at 60–720 periods (std. dev. 1.9 Sv, excluding the seasonal cycle) is comparable to geostrophic interior oceanic variability estimated at similar periods at 26° N attributed to eddy activity (std. dev. 2.5 Sv, Kanzow et al., 2009) and westward Rossby wave propagation (std. dev. 2.3 Sv, Hirschi et al., 2007). Transport variability driven by westward propagating baroclinic upper-ocean eddies has also been observed to modulate the Antilles Current east of the Florida Straits at timescales of several months (Lee et al., 1996; Halliwell et al., 1991; Johns et al., 2008), although the blocking effect of topography may limit the effects of similar eddies on the Florida Current (Anderson and Corry, 1985b). Another possible source of variability may be southward propagating shelf waves. Evidence of coherent changes in sea surface height along the western Atlantic margin that may be related to such signals has been found (Hughes and Meredith, 2006), however model studies suggest that at sub-interannual timescales AMOC variability at 26° N is not obviously coherent with AMOC changes at other latitudes (e.g. Hirschi et al., 2007; Bingham et al., 2007) because local transport variability is thought to obscure meridional signals that may facilitate basin scale changes (Johnson and Marshall, 2002). Greatbatch et al. (1995) found sub-annual Florida Straits transport variability of baroclinic origin in the WOCE-CME model though no particular source was identified; the authors highlight northward advection of density anomalies in the Florida Current as a further possible source of variability to those mentioned above.

4.3 Relationship of Florida Straits, Ekman and Sverdrup transport variability to AMOC variability

The Florida Straits and Ekman transports combined comprise almost the entire northward flow of water at 26° N. These components, combined with mooring measurements of geostrophic Upper Mid-Ocean Transport (UMOT), are used by the RAPID-WATCH array to continuously measure AMOC variability at 26° N at periods greater than 10 days (e.g. Cunningham et al., 2007; Kanzow et al., 2007, 2010). Four years of measurements by RAPID-WATCH has revealed that Gulf Stream, Ekman and UMOT variability are uncorrelated and therefore at sub-annual and seasonal timescales these components contribute independently to AMOC variability (defined as the meridional overturning streamfunction maximum). The Gulf Stream (Florida Straits) and Ekman transport variability discussed in this study at these timescales can therefore be considered to contribute directly to AMOC variability at 26° N.

Theoretically, northward Florida Straits and Ekman transport added to southward Sverdrup transport could provide an index of MOC strength at 26° N, though this relies on simple dynamics that may not hold in the real ocean. From 2004–2008, UMOT variability shows a correlation with NCEP Sverdrup transports (both low passed at 30-day period) of $r = 0.28$, however no correlation is observed once seasonal cycles are removed. It is not yet clear at what periods Sverdrup transport variability may (if at all) reflect observed UMOT variability. At sub-annual timescales eddy activity is observed to be both modified and diminished approaching the western margin (Kanzow et al., 2009). The seasonal cycle of UMOT shows no evidence of a semi-annual component comparable to that seen for Sverdrup transport. Indeed, the UMOT transport seems to possess a dominant annual cycle driven locally by wind stress curl close to the eastern Atlantic margin (Kanzow et al., 2010) which is not resolved by the NCEP, NOC v1.1 and IFREMER MWF QuikSCAT climatologies. The absence of a similar semi-annual cycle in RAPID-WATCH observations is not surprising for at semi-annual timescale, the mid-ocean at 26° N should adjust barotropically which is effectively invisible to the RAPID-WATCH array.

Bryden et al. (2005) compared five hydrographic sections at 25° N to suggest a 30% slowing of the AMOC between 1957 and 2004; whilst northward Gulf Stream transport remained nearly constant, in 2004 more Gulf Stream flow appeared to recirculate back southward in the sub-tropical gyre thermocline and less returned southward at depth. Assuming Gulf Stream and Ekman transport remain constant, a long term decrease in NCEP southward Sverdrup transports of 1 Sv (Sect. 3.3) seems to imply a long term strengthening of the AMOC from 1950 to present, in disagreement with the Bryden et al. (2005) result. However, changes in mid-ocean thermocline circulation may not necessarily be constrained by Sverdrup

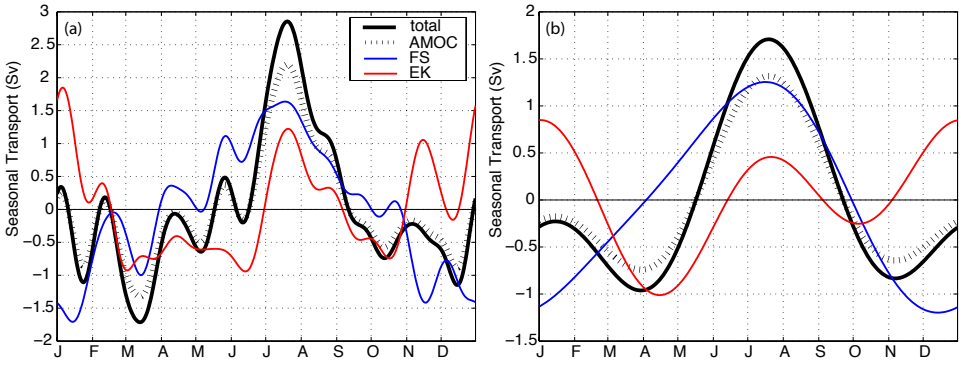

Fig. 12. Seasonal cycles of Florida Straits transport (blue), Ekman transport (red), Ekman and Florida Straits total (black) and projection on AMOC (dashed black; assumes barotropic compensation of combined transport). **(a)** 30-day low-pass mean daily transports (see Fig. 2); Florida Straits, Ekman, Total and AMOC seasonal range = 3.3 Sv, 2.8 Sv, 4.6 Sv and 3.5 Sv respectively, **(b)** combined annual and semi-annual harmonics (see Fig. 3); Florida Straits, Ekman, Total and AMOC seasonal range = 2.5 Sv, 1.9 Sv, 2.7 Sv and 2.1 Sv respectively.

dynamics (de Boer and Johnson, 2007; Longworth, 2007), hydrographic measurements of upper-ocean transport variability may be more susceptible to shorter term variability than previously thought (Kanzow et al., 2010) and reliability of decadal Sverdrup transport trends is not clear (Sect. 3.3). On interannual and longer scales, Florida Straits transport variability (observed to be up to ≈2 Sv in amplitude) may respond to changes in wind-stress curl over the sub-tropical gyre (DiNezio et al., 2009). If Sverdrup balance does hold at these timescales then, in the absence of mid-ocean transport observations, our ability to determine long-term trends in the AMOC may be limited by the reliability of wind stress climatologies.

4.3.1 Contribution of Florida Straits and Ekman transports to seasonal AMOC and heat transports

Four years of observations by the RAPID-WATCH array has revealed that the AMOC at 26° N possesses a substantial seasonal cycle (Kanzow et al., 2010), thus the Florida Straits and Ekman transports are now considered in terms of their seasonal projection on the AMOC. Figure 12a shows the combined seasonal transport of the Florida Straits and Ekman transports along with their projection on the AMOC assuming they are barotropically compensated (where compensating barotropic flow is assumed from the surface to 4800 m, and AMOC streamfunction maxima is taken as 1100 m). Barotropic compensation of Ekman transport variability has been demonstrated in several studies (e.g. Jayne and Marotzke, 2001; Kanzow et al., 2007) whilst bottom pressure measurements east of the Florida Straits (available to 4800m depth) suggest that Florida Straits transport variability is compensated locally by a barotropic transport adjacent to the continental shelf (Bryden et al., 2009). The seasonal cycles combined project on the AMOC with expected long-term seasonal cycle range of 3.5 Sv. Figure 12b also shows the projection of the combined annual and semi-annual Florida Straits and Ekman transport harmonics only on the AMOC, which have a long-term seasonal cycle range of 2.1 Sv. The defined July maxima arises when the dominant annual and semi-annual cycles of the Florida Straits and Ekman transports respectively come into phase in Summer.

Using the seasonal transports shown in Fig. 12a, seasonal meridional heat transport is also calculated for Florida Straits and Ekman transports at 26° N. For each transport:

$$Q_{\text{net}} = \rho c_p V_n \theta_n - \rho c_p V_s \theta_s, \quad (4)$$

where Q_{net} = seasonal net heat transport for the Florida Straits or Ekman (J s^{-1}), V =seasonal meridional transport (Sv), θ = seasonal transport weighted potential temperature of meridional flow (°C), ρ = density of seawater (taken as $1025\,\text{kg m}^{-3}$), c_p = specific heat of seawater ($3994\,\text{J kg}^{-1}\,^{\circ}\text{C}^{-1}$) and subscripts "$n$" and "$s$" refer to northward and compensating southward flows. See Appendix A for further details. Both Florida Straits and Ekman seasonal heat transports at 26° N have similar structure to their respective seasonal mass transports shown in Fig. 12a. This occurs because both seasonal heat transports are chiefly attributable to seasonal advection of the mean temperature field, though the contributions made by seasonal temperature variations (advected in the mean flow) are not negligible, particularly in the Florida Straits. The seasonal range of Florida Straits, Ekman and combined heat transports at 26° N is 0.25 PW, 0.20 PW and 0.40 PW respectively.

It is notable that the Ekman and Florida Straits seasonal heat transport cycles are similar in magnitude at 26° N. However, because the calculation of seasonal Ekman and Florida Straits heat transport variability assumes mass transport compensation identical in structure to that of sub-annual transport variability, large amounts of non-seasonal noise is also expected in their heat transport timeseries, as seen for the timeseries of mass transport.

5 Summary

The successful deployment of the RAPID-WATCH array has placed significant emphasis on the AMOC at 26° N. To date the array has successfully measured the strength of the AMOC for 5 years and already a strong seasonal cycle seems to be emerging (Kanzow et al., 2010). Whilst ongoing measurements of geostrophic transport across the ocean interior at 26° N remain somewhat in their infancy, high quality decadal length datasets of Florida Straits and surface wind stress are available. In this study the seasonal cycles and variability of the Florida Straits, Ekman and Sverdrup transports at 26° N have been analysed with the intention of complementing and enhancing the understanding of the AMOC based on observations made by the RAPID-WATCH array. The main conclusions of this study are as follows:

- The mean seasonal cycle of the Florida Straits transport shows a clear annual periodicity with a maxima in mid-July, a minima in mid-January and a range of 3.3 Sv. Both modern wind stress climatologies and data from a 1/4° eddy-permitting model support previous studies that suggest the seasonal cycle is set by meridional wind stress downstream and local to the Florida straits. The seasonal cycle only emerges from decadal length observations whereas over shorter observational periods calculations of the seasonal cycle are obscured by stochastic variability.

- At periods < 10 days, observed Florida Straits transport variability shows coherence with along channel climatological wind stress. At periods of 10–70 days, model data highlights a significant role for surface wind forcing in driving transport variability though the exact mechanism(s) remain unexplained. At periods of 60–720 days (excluding annual), observed Florida Straits transport variability shows no significant coherence with North Atlantic wind stress (including the NAO index). This is supported by model data which suggests that at ≈70–1000 day periods, internal ocean variability (i.e. variability not directly forced by changes in surface winds and buoyancy) contributes significantly to Florida Straits transport variability. At interannual and longer periods, Florida Straits transport variability may reflect changes in strength of the sub-tropical gyre and thermohaline circulation.

- The mean seasonal cycle of Ekman transport at 26° N shows no dominant annual or semi-annual periodicity and instead comprises several maxima and minimaof maximum range 2.8 Sv. This is largely due to differing seasonal transport regimes east and west of 50–60° W. Similar to Florida Straits transports, the Ekman transport seasonal cycle only emerges from decadal length observations. Ekman transports show significant coherence with the NAO at seasonal to decadal periods; a change of ≈+1 Sv per NAO index unit is observed. Around 60% of both sub-annual and interannual Ekman transport variability occurs in phase across 26° N which is partly attributable to the NAO. This contributes to enhanced section-wide Ekman transport variability during the winter months when the NAO is at its strongest.

- The mean seasonal cycle of Sverdrup transport at 26° N shows clear section-wide semi-annual periodicity with a maximum range 20.4 Sv which is strongly persistent (particularly in terms of phase) from year to year. Sverdrup transports show little coherence with the NAO at sub-decadal periods though at decadal timescales a change of ≈+4–5 Sv per NAO index unit is possible. No dominant modes of Sverdrup transport variability are found across 26° N such that Sverdrup transport variability appears less spatially coherent (more localised longitudinally and latitudinally) than for Ekman transports.

- At 26° N, Florida Straits and Ekman transports project on the AMOC with a combined seasonal cycle range of 3.5 Sv. The combined range of seasonal heat transport is 0.40 PW. Because Florida Straits and Ekman heat transports are expected to be strongly correlated with their mass transports, their seasonal heat transports will only emerge from decadal length observations.

Appendix A

Heat transport calculations

For Florida Straits heat transport, the term $\rho c_p V_n \theta_n$ takes V_n to be the seasonal transport (Fig. 12, red line + mean transport of 32.1 Sv) and θ_n as the mean annual cycle of observed Florida Current flow weighted temperature (min. 19.05 °C, max. 19.67 °C, see Shoosmith et al., 2005, Fig. 4). For Ekman transport, $\rho c_p V_n \theta_n$ takes V_n to be the seasonal transport (Fig. 12, blue line + mean transport of 3.6 Sv) and θ_n as the mean seasonal cycle of Ekman layer (surface to 100 m) potential temperature at 26° N computed using the Hydrobase 2 database (a seasonally averaged hydrographic climatology, http://www.whoi.edu/science/PO/hydrobase). Note that monthly Hydrobase Ekman layer temperatures are converted to daily values using cubic spline interpolation giving a smooth annual cycle of range 3.3 °C (September maxima = 24.9 °C, March minima = 21.6 °C).

For the barotropic return flows of northwards Florida Straits and Ekman transports, $V_s = V_n$ to maintain mass balance. For the Florida Straits return flow, θ_s is taken as the mean seasonal potential temperature of seawater adjacent to the Bahamian continental shelf calculated combining RAPID-WATCH mooring data from 100–4800 m (www.noc.soton.ac.uk/rapidmoc, April 2004–April 2007) and Hydrobase 2 Ekman layer temperature (as above) where

mooring data is patchy. For the Ekman return flow, θ_s is taken as the mean seasonal potential temperature of seawater in the basin interior from 0–4800 m at 26° N, calculated using Hydrobase 2 (monthly interior Hydrobase 2 temperatures are converted to daily values using cubic spline interpolation, as for Ekman layer temperatures). θ_s has a mean of 5.41 °C and 5.62 °C for the Florida Straits and Ekman transport return flows respectively. The seasonal range of θ_s in both cases is small, <0.2 °C.

Acknowledgements. The Florida Current cable and section data are made freely available on the Atlantic Oceanographic and Meteorological Laboratory web page (www.aoml.noaa.gov/phod/floridacurrent/) and are funded by the NOAA Office of Climate Observations. NOAA NCEP-NCAR reanalysis data are freely available via the IRI/LDEO Climate Data Library (http://iridl.ldeo.columbia.edu/). NOC v1.1 climatology data are freely available via the NOC/OOC website (http://www.noc.soton.ac.uk/noc_flux/noc1_1.php). The IFREMER MWF QuikSCAT product is made freely available on the IFREMER ftp server (ftp.ifremer.fr/ifremer/cersat/products/gridded/mwf-quikscat/). NAO index data are freely distributed by NOAA's Climate Prediction Center (http://www.cpc.noaa.gov/products/precip/CWlink/pna/nao.shtml). Data from the RAPID-WATCH MOC monitoring project are funded by the Natural Environment Research Council (NERC) and are freely available from www.noc.soton.ac.uk/rapidmoc.

The authors would like to thank B. A. de Cuevas and A. T. Blaker (NOC, Southampton, UK) for their assistance with NEMO model data, C. S. Meinen (NOAA/AOML, Miami, USA) for assistance with Florida Straits transport analysis and D. R. Shoosmith (BAS, Cambridge, UK) for kindly providing Florida Straits temperature data. H. L. Bryden and J. J.-M. Hirschi thank NERC for ongoing support of their research efforts. C. P. Atkinson was supported by a NERC PhD studentship.

Edited by: D. Stevens

References

Anderson, D. L. T. and Corry, R. A.: Seasonal transport variations in the Florida Straits – A model study, J. Phys. Oceanogr., 15, 773–786, 1985a.

Anderson, D. L. T. and Corry, R. A.: Ocean response to low-frequency wind forcing with application to the seasonal-variation in the Florida Straits Gulf-Stream transport, Prog. Oceanogr., 14, 7–40, 1985b.

Baringer, M. O. and Larsen, J. C.: Sixteen years of Florida Current transport at 27°N, Geophys. Res. Lett., 28, 3179–3182, 2001.

Barnier, B., Madec, G., Penduff, T., Molines, J. M., Treguier, A. M., Le Sommer, J., Beckmann, A., Biastoch, A., Boning, C., Dengg, J., Derval, C., Durand, E., Gulev, S., Remy, E., Talandier, C., Theetten, S., Maltrud, M., McClean, J., and De Cuevas, B.: Impact of partial steps and momentum advection schemes in a global ocean circulation model at eddy-permitting resolution, Ocean Dynam., 56, 543–567, doi:10.1007/s10236-006-0082-1, 2006.

Barnston, A. G. and Livezey, R. E.: Classification, seasonality and persistence of low-frequency atmospheric circulation patterns, Mon. Weather Rev., 115, 1083–1126, 1987.

Beal, L. M., Hummon, J. M., Williams, E., Brown, O. B., Baringer, W., and Kearns, E. J.: Five years of Florida Current structure and transport from the Royal Caribbean Cruise Ship Explorer of the Seas, J. Geophys. Res., 113, C06001, doi:10.1029/2007JC004154, 2008.

Bingham, R. J., Hughes, C. W., Roussenov, V., and Williams, R. G.: Meridional coherence of the North Atlantic meridional overturning circulation, Geophys. Res. Lett., 34, L23606, doi:10.1029/2007GL031731, 2007.

Boning, C. W., Doscher, R., and Budich, R. G.: Seasonal transport variation in the western subtropical North-Atlantic - Experiments with an eddy-resolving model, J. Phys. Oceanogr., 21, 1271–1289, 1991.

Bryden, H. L., Longworth, H. R., and Cunningham, S. A.: Slowing of the Atlantic meridional overturning circulation at 25°N, Nature, 438, 655–657, doi:10.1038/nature04385, 2005.

Bryden, H. L., Mujahid, A., Cunningham, S. A., and Kanzow, T.: Adjustment of the basin-scale circulation at 26°N to variations in Gulf Stream, deep western boundary current and Ekman transports as observed by the Rapid array, Ocean Sci., 5, 421–433, 2009,
http://www.ocean-sci.net/5/421/2009/.

Cunningham, S. A., Kanzow, T., Rayner, D., Baringer, M. O., Johns, W. E., Marotzke, J., Longworth, H. R., Grant, E. M., Hirschi, J. J. M., Beal, L. M., Meinen, C. S., and Bryden, H. L.: Temporal variability of the Atlantic meridional overturning circulation at 26.5°N, Science, 317, 935–938, doi:10.1126/science.1141304, 2007.

de Boer, A. M. and Johnson, H. L.: Inferring the zonal distribution of measured changes in the meridional overturning circulation, Ocean Sci., 3, 55–57, doi:10.5194/os-3-55-2007, 2007.

DiNezio, P. N., Gramer, L. J., Johns, W. E., Meinen, C. S., and Baringer, M. O.: Observed Interannual Variability of the Florida Current: Wind Forcing and the North Atlantic Oscillation, J. Phys. Oceanogr., 39, 721–736, doi:10.1175/2008JPO4001.1, 2009.

Emery, W. J. and Thomson, R. E.: Data analysis methods in physical oceanography, Elsevier, 2nd edn., 2001.

Fanning, A. F., Greatbatch, R. J., DaSilva, A. M., and Levitus, S.: Model-calculated seasonal transport variations through the Florida Straits - A comparison using different wind-stress climatologies, J. Phys. Oceanogr., 24, 30–45, 1994.

Fiechter, J. and Mooers, C. N. K.: Simulation of frontal eddies on the East Florida Shelf, Geophys. Res. Lett., 30, 2151, doi:10.1029/2003GL018307, 2003.

Greatbatch, R. J. and Goulding, A.: Seasonal variations in a linear barotropic model of the North Atlantic driven by the Hellerman and Rosenstein wind stress-field, J. Phys. Oceanogr., 19, 572–595, 1989.

Greatbatch, R. J., Lu, Y. Y., DeYoung, B., and Larsen, J. C.: The variation of transport through the Straits of Florida - A barotropic model study, J. Phys. Oceanogr., 25, 2726–2740, 1995.

Grist, J. P., Josey, S. A., Marsh, R., Good, S. A., Coward, A. C., de Cuevas, B. A., Alderson, S. G., New, A. L., and Madec, G.: The roles of surface heat flux and ocean heat transport convergence in determining Atlantic Ocean temperature variability, Ocean Dynam., 60, 771–790, doi:10.1007/s10236-010-0292-4, 2010.

Halliwell, G. R., Ro, Y. J., and Cornillon, P.: Westward propagating SST anomalies and baroclinic eddies in the Sargasso Sea, J. Phys.

Oceanogr., 21, 1664–1680, 1991.
Hirschi, J. J. M., Killworth, P. D., and Blundell, J. R.: Subannual, seasonal, and interannual variability of the North Atlantic meridional overturning circulation, J. Phys. Oceanogr., 37, 1246–1265, doi:10.1175/JPO3049.1, 2007.
Hughes, C. W. and Meredith, C. P.: Coherent sea-level fluctuations along the global continental slope, Philos. T. R. Soc. A, 364, 885–901, doi:10.1098/rsta.2006.1744, 2006.
Hurrell, J. W. and Deser, C.: North Atlantic climate variability: The role of the North Atlantic Oscillation, J. Marine Syst., 78, 28–41, doi:10.1016/j.jmarsys.2008.11.026, 2009.
Hurrell, J. W., Kushnir, Y., Ottersen, G., and Visbeck, M.: The North Atlantic Oscillation: Climate Significance and Environmental Impact, Eds. Geophysical Monograph Series, 134, 279 pp, 2003.
Hurrell, J. W., Visbeck, M., Busalacchi, A., Clarke, R. A., Delworth, T. L., Dickson, R. R., Johns, W. E., Koltermann, K. P., Kushnir, Y., Marshall, D., Mauritzen, C., McCartney, M. S., Piola, A., Reason, C., Reverdin, G., Schott, F., Sutton, R., Wainer, I., and Wright, D.: Atlantic climate variability and predictability: A CLIVAR perspective, J. Climate, 19, 5100–5121, 2006.
IPCC: Climate Change 2007: The Physical Science Basis. Contribution of working group 1 to the fourth assessment report of the IPCC, Cambridge University Press, 2007.
Jayne, S. R. and Marotzke, J.: The dynamics of ocean heat transport variability, Rev. Geophys., 39, 385–411, 2001.
Johns, W. E. and Schott, F.: Meandering and transport variations of the Florida Current, J. Phys. Oceanogr., 17, 1128–1147, 1987.
Johns, W. E., Beal, L. M., Baringer, M. O., Molina, J. R., Cunningham, S. A., Kanzow, T., and Rayner, D.: Variability of shallow and deep western boundary currents off the Bahamas during 2004-05: Results from the 26°N RAPID-MOC array, J. Phys. Oceanogr., 38, 605–623, doi:10.1175/2007JPO3791.1, 2008.
Johnson, H. L. and Marshall, D. P.: A theory for the surface Atlantic response to thermohaline variability, J. Phys. Oceanogr., 32, 1121–1132, 2002.
Josey, S. A., Kent, E. C., and Taylor, P. K.: Wind stress forcing of the ocean in the SOC climatology: Comparisons with the NCEP-NCAR, ECMWF, UWM/COADS, and Hellerman and Rosenstein Datasets, J. Phys. Oceanogr., 32, 1993–2019, 2002.
Kalnay, E., Kanamitsu, M., Kistler, R., Collins, W., Deaven, D., Gandin, L., Iredell, M., Saha, S., White, G., Woollen, J., Zhu, Y., Chelliah, M., Ebisuzaki, W., Higgins, W., Janowiak, J., Mo, K. C., Ropelewski, C., Wang, J., Leetmaa, A., Reynolds, R., Jenne, R., and Joseph, D.: The NCEP/NCAR 40-year reanalysis project, B. Am. Meteorol. Soc., 77, 437–471, 1996.
Kanzow, T., Cunningham, S. A., Rayner, D., Hirschi, J. J. M., Johns, W. E., Baringer, M. O., Bryden, H. L., Beal, L. M., Meinen, C. S., and Marotzke, J.: Observed flow compensation associated with the MOC at 26.5°N in the Atlantic, Science, 317, 938–941, doi:10.1126/science.1141293, 2007.
Kanzow, T., Johnson, H. L., Marshall, D. P., Cunningham, S. A., Hirschi, J. J. M., Mujahid, A., Bryden, H. L., and Johns, W. E.: Basinwide Integrated Volume Transports in an Eddy-Filled Ocean, J. Phys. Oceanogr., 39, 3091–3110, doi:10.1175/2009JPO4185.1, 2009.
Kanzow, T., Cunningham, S. A., Johns, W. E., Hirschi, J. J. M., Marotzke, J., Baringer, M. O., Meinen, C. S., Chidichimo, M. P., Atkinson, C. P., Beal, L. M., Bryden, H. L., and Collins, J.: Seasonal variability of the Atlantic meridional overturning circulation at 26.5° N, J. Climate, doi:10.1175/2010JCLI3389.1, in press, 2010.
Kistler, R., Kalnay, E., Collins, W., Saha, S., White, G., Woollen, J., Chelliah, M., Ebisuzaki, W., Kanamitsu, M., Kousky, V., van den Dool, H., Jenne, R., and Fiorino, M.: The NCEP-NCAR 50-year reanalysis: Monthly means CD-ROM and documentation, B. Am. Meteorol. Soc., 82, 247–267, 2001.
Larsen, J. C.: Transport and heat-flux of the Florida Current at 27°N derived from cross-stream voltages and profiling data - Theory and observations, Philos. T. Roy. Soc. A, 338, 169–236, 1992.
Leaman, K. D., Molinari, R. L., and Vertes, P. S.: Structure and variability of the Florida Currentat 27°N: April 1982-July 1984, J. Phys. Oceanogr., 17, 565–583, 1987.
Lee, T. N. and Williams, E.: Wind-forced transport fluctuations of the Florida Current, J. Phys. Oceanogr., 18, 937–946, 1988.
Lee, T. N., Yoder, J. A., and Atkinson, L. P.: Gulf-Stream frontal eddy influence on productivity of the southeast United-States continental-shelf, J. Geophys. Res., 96, 22191–22205, 1991.
Lee, T. N., Johns, W. E., Zantopp, R. J., and Fillenbaum, E. R.: Moored observations of western boundary current variability and thermohaline circulation at 26.5°N in the subtropical north Atlantic, J. Phys. Oceanogr., 26, 962–983, 1996.
Longworth, H. R.: Constraining variability of the Atlantic Meridional Overturning Circulation at 25°N from historical observations, 1980-2005, Ph.D. thesis, School of Ocean and Earth Science, University of Southampton, Southampton, UK, 200 pp., 2007.
Madec, G., Delecluse, P., Imbard, M., and Levy, C.: OPA 8.1 ocean general circulation model reference manual, IPSL Tech. Rep. 11, Institut Pierre-Simon Laplace, 2008.
Marshall, J., Kushner, Y., Battisti, D., Chang, P., Czaja, A., Dickson, R., Hurrell, J., McCartney, M., Saravanan, R., and Visbeck, M.: North Atlantic climate variability: Phenomena, impacts and mechanisms, Int. J. Climatol., 21, 1863–1898, doi:10.1002/joc.693, 2001.
Mayer, D. A. and Weisberg, R. H.: A description of COADS surface meteorological fields and the implied Sverdrup transports for the Atlantic Ocean from 30°S to 60°N, J. Phys. Oceanogr., 23, 2201–2221, 1993.
Meinen, C. S., Baringer, M. O., and Garcia, R. F.: Florida Current transport variability: an analysis of annual and longer-period signals, Deep-Sea Res. Pt. I, 57, 835–846, 2010.
Molinari, R. L., Maul, G. A., Chew, F., Wilson, W. D., Bushnell, M., Mayer, D., Leaman, K., Schott, F., Lee, T., Zantopp, R., Larsen, J. C., and Sandford, T. B.: Sub-tropical Atlantic climate studies – Introduction, Science, 227, 292–295, 1985.
Risien, C. M. and Chelton, D. B.: A Global Climatology of Surface Wind and Wind Stress Fields from Eight Years of QuikSCAT Scatterometer Data, J. Phys. Oceanogr., 38, 2379–2413, doi:10.1175/2008JPO3881.1, 2008.
Rosenfeld, L. K., Molinari, R. L., and Leaman, K. D.: Observed and modeled annual cycle of transport in the Straits of Florida and east of Abaco-Island, The Bahamas (26.5°N), J. Geophys. Res., 94, 4867–4878, 1989.
Schmitz, W. J. and Richardson, P. L.: On the sources of the Florida Current, Deep-Sea Res. Pt. I, 38, S379–S409, 1991.
Schott, F. and Zantopp, R.: Florida Current - Seasonal and interannual variability, Science, 227, 308–311, 1985.

Schott, F. A., Lee, T. N., and Zantopp, R.: Variability of structure and transport of the Florida Current in the period range of days to seasonal, J. Phys. Oceanogr., 18, 1209–1230, 1988.

Shoosmith, D. R., Baringer, M. O., and Johns, W. E.: A continuous record of Florida Current temperature transport at 27°N, Geophys. Res. Lett., 32, L23603, doi:10.1029/2005GL024075, 2005.

Sime, L. C., Stevens, D. P., Heywood, K. J., and Oliver, K. I. C.: A decomposition of the Atlantic meridional overturning, J. Phys. Oceanogr., 36, 2253–2270, 2006.

Vellinga, M. and Wood, R. A.: Global climatic impacts of a collapse of the Atlantic thermohaline circulation, Climatic Change, 54, 251–267, 2002.